1970

The electronic heat capacity of Re03

David Anthony Keller
Iowa State University

THE ELECTRONIC HEAT CAPACITY OF ReO_3

by

David Anthony Keller

A Dissertation Submitted to the
Graduate Faculty in Partial Fulfillment of
The Requirements for the Degree of
DOCTOR OF PHILOSOPHY

Major Subject: Physical Chemistry

Approved:

Signature was redacted for privacy.

In Charge of Major Work

Signature was redacted for privacy.

Head of Major Department

Signature was redacted for privacy.

Dean of Graduate College

Iowa State University
Ames, Iowa

1970

TABLE OF CONTENTS

LIST OF TABLES

LIST OF FIGURES

I. INTRODUCTION

Heat capacity work in Physical and Inorganic Group VI had, prior to 1969, been limited to measurements above $4^{o}K$, utilizing relatively standard adiabatic calorimetry (1), with an accuracy of about .1% at $30^{o}K$, decreasing to about 50% at $4^{o}K$, due primarily to the limitations of Pt thermometry. A couple of the compounds studied ($HoCl_3 \cdot 6H_2O$ (2), $TbCl_3 \cdot 6H_2O$ (2)) exhibited Schottky bumps in the heat capacity in the neighborhood of $4^{o}K$.

Magnetic susceptibility studies in Group VI spanned the range $1.2\text{-}300^{o}K$, and here also interesting peaks appeared in the neighborhood of $4^{o}K$ (in $CsNiCl_3$ (3), and $NiC_4O_4 \cdot 2H_2O$ (4)).

At the same time theoretical work (5) in Group VI on electrical transport in metal oxide systems led to predictions that could partially be verified by heat capacity work below $4^{o}K$.

In order to provide an instrument to study thermal behavior of compounds like those mentioned above at $T \leq 4^{o}K$, as well as to provide an instrument capable of more accurate (by at least a factor of five) heat capacity measurements in the temperature range $4\text{-}20^{o}K$, the construction of a He-3 calorimeter operable in the range $.4\text{-}20^{o}K$ was carried out as described herein.

While calorimetric techniques in the range $.4\text{-}20^{o}K$ are becoming somewhat standardized, the requirements are still

rather formidable. For example, heat capacity measurements below $4^{o}K$ require relatively simple shielding of the sample from radiation. In many cases no shielding is used other than that provided by the walls which separate the sample from the cooling baths. However, at $15^{o}K$ the radiative heat leak is large enough to require either "adiabatic" shielding, or some other type of temperature controlled shield. Also, heat leaks through thermometer and heater leads, which may be avoided by use of superconducting leads below $4^{o}K$, may not be so avoided at $20^{o}K$ with materials presently available. Further, in practice all thermometry in the range $.4\text{-}20^{o}K$ requires calibration with reference to gas thermometry, either directly or through a secondary standard. In the range $.4\text{-}4^{o}K$ several secondary standards are conveniently available which cover all or part of the range, namely the vapor pressure of liquid He-4, the vapor pressure of liquid He-3, and the magnetic susceptibility of certain paramagnetic salts, such as cerous magnesium nitrate (CMN). However, in the range $4\text{-}20^{o}K$ thermometer calibration is very inconvenient because it usually requires gas thermometry, unless one has access to a doped Ge thermometer which has been well calibrated against a primary standard. In summary, the design of one instrument to cover heat capacities in the range $.4\text{-}20^{o}K$ requires a "hybridization" of techniques used above $20^{o}K$ with those used below $4^{o}K$.

The project chosen for the initial use of the He-3 calorimeter was the measurement of the heat capacity of ReO_3 from

~.4-4°K. This study was undertaken for several reasons.

First, ReO_3 is a simple prototype for the cubic perovskites (ABO_3), as shown by Karian (5). In general, the perovskites are of interest to solid state research because they display a wide range of properties (e.g. from diamagnetic to ferromagnetic, from dielectric to ferroelectric, from electrically insulating to conducting) (6), and further because they have shown promise as laser host materials, as laser modulators, and as infrared windows (6).

Second, ReO_3 has been treated theoretically in Group VI (5) and elsewhere (7) by two different band theory approaches, which predicted quite different low temperature heat capacity results.

Finally, vapor transported ReO_3 has recently become available in sufficient quantities from Physics Group VI to allow heat capacity studies.

II. LITERATURE SURVEY

A. Calorimetry from .4-20°K

He-4 was first liquefied in 1908 (8), and in 1914 Kamerlingh Onnes at Leiden made the first heat capacity measurement in the liquid He-4 temperature region (9). His objective was to determine if there was an "anomaly" in the heat capacity of Hg as it became superconducting. He concluded there was none. In 1928 Keesom and Andrews measured the heat capacity of lead from 2-17°K, using more advanced techniques than Onnes, again to search for an "anomaly" as the sample became superconducting. They (10) reached the same conclusion as Onnes.

At the present time it is well known that there is a pronounced "anomaly" in the heat capacity in going through a superconducting transition (11). Obviously experimental techniques have improved since Keesom's work. Lower temperatures can be reached, and much more accurate measurements can be made. A number of review articles (12,13,14) and books (15, 16,17) document the evolution of present day calorimetric techniques used in the range .4-20°K, and efforts are still being made to further improve techniques, especially in thermometry (18).

In spite of the demanding experimental requirements, calorimetry below 15°K has contributed significantly to a wide variety of studies. Some of the areas of study, along with exemplary calorimetric references, are superconductivity

(11), lattice vibrations (19), magnetic transitions (19), hyperfine interactions (19), crystal field theory (19,20), quadrupole interactions (19,21), critical phenomena (22), verification of the 3rd Law of Thermodynamics (23), macroscopic quantum effects (24), magnetic impurity scattering (25), van der Waals-type bonding (26), surface effects (27), electron-phonon interactions (28), and band theory (29).

B. Electronic Heat Capacity

In 1928 Sommerfeld (30) treated "free" electrons, which were assumed to exist in metallic substances, with quantum statistics. His results predicted that under certain conditions the "free" electrons would contribute a term to the heat capacity which was linear with respect to temperature, i.e.

$$C_v^e = \gamma T \qquad (1)$$

where C_v^e is the molar "free" electron heat capacity at constant volume (commonly referred to as the electronic heat capacity), γ is a constant, and T is absolute temperature. Later in 1934 Bethe and Sommerfeld (31) elaborated further on the subject of "free" electron theory, and presented the equation

$$C_v^e = (2/3)\pi^2 k^2 N(E_F) T \text{ for } T \ll E_F/k \qquad (2)$$

where k is Boltzmann's constant, and $N(E_F)$ is the density of energy states at the Fermi energy, E_F. From simple band theory (32) it can be shown that for "free" electrons

$$N(E_F) = 2\pi(2m)^{3/2}\ V\ h^{-3}\ E_F^{1/2} \qquad (3)$$

where m is the "free" electron rest mass, h is Planck's constant, and

$$E_F = (1/8m)(3nh^3/\pi V)^{2/3} \qquad (4)$$

where n is the number of "free" electrons in a sample of molar volume, V. Substituting Equations 3 and 4 into Equation 2 leads to

$$C_V^e = (4\pi^3k^2/3h^2)(3nV^2/\pi)^{1/3}mT \qquad (5)$$

for one mole of sample.

At liquid He-4 temperatures the total molar heat capacity, C_V, of many materials is given by

$$C_V = \gamma T + \beta T^3 \qquad (6)$$

where γ and β are constants. The first term is the electronic contribution to the heat capacity, and the second term is the lattice contribution. From Equation 6 it can be seen that a plot of C_V/T versus T^2 yields a straight line with slope β and intercept γ. Hence the electronic term can be measured and compared with theoretical predictions. Generally the measured value has not agreed with the "free" electron value predicted by Equation 5, and frequently m has been adjusted to provide agreement, with the new value of m labelled as the "effective" electron mass, m*.

More recent theoretical investigations have sought to calculate $N(E_F)$ directly, and using Equation 2, compare theory with experiment. Again the agreement has not been

good and new concepts such as electron-phonon enhancement have been introduced to accound for the discrepancy. Referenced discussions of the above developments in electronic heat capacity have appeared in review articles by Daunt (33), Keesom (34), and Parkinson (35), and elsewhere (36,19).

C. ReO_3

As mentioned in the INTRODUCTION, ReO_3 has served as a prototype for the cubic perovskites. This similarity can be visually appreciated by comparing the known (37) crystal structure of ReO_3 with that of a cubic perovskite (ABO_3) (6). Figure 1 shows the cubic perovskite structure. The ReO_3 structure is obtained by substituting rhenium for B, and removing the A atom from the body center.

The electrical conductivity of ReO_3 has been measured and found to be roughly one-tenth that of Cu at room temperature (38). Optical properties were measured (39) and discussed in terms of several band models that had been proposed earlier. The de Haas-van Alphen effect in ReO_3 was measured by Marcus (40), and the NMR of Re-185 and Re-187 in ReO_3 was measured by Narath and Barham (41), who concluded that the conduction band was predominantly made up of d electron orbitals.

An article was published by Honig et al. (42) outlining how a tight binding calculation might be made for ReO_3. It was suggested that such a calculation would resolve the

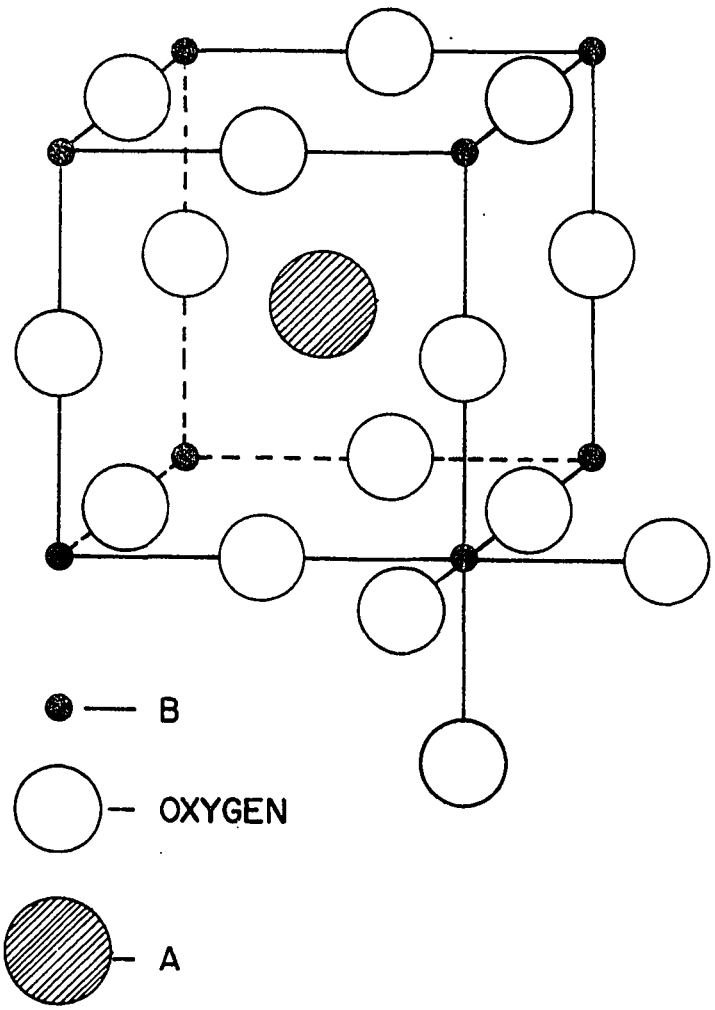

Fig. 1. Crystal structure of a cubic peroskite, ABO_3

problem of the nature of the conduction band. Such a calculation was made by Karlan (5), and a conduction model proposed. Another band theory calculation for ReO_3 was made by Mattheiss (7), using the APW method at symmetry points in the Brillouin zone, and the Slater-Koster tight binding interpolation scheme for intermediate points. The models of Karlan and Mattheiss differ appreciably in the shape of the density of states curve, the Fermi energy, and the contribution of particular orbitals to the conduction band.

III. EXPERIMENTAL EQUIPMENT

A. Calorimeter

1. General description

Heat capacity measurements below room temperature usually involve cooling the sample-plus-addenda (SPA) to the lowest temperature desired, thermally isolating the SPA from the cooling baths, adding a measured amount of heat to the SPA, and determining the temperature increase due to the heat input. The last two steps are repeated a number of times until the highest desired temperature is reached. After analyzing the results to obtain the heat capacity of the SPA, the entire procedure is repeated for the addenda alone, and the difference between the two measurements yields the heat capacity of the sample.

The main body of the apparatus used to carry out the above outlined procedure is shown schematically in Fig. 2. Table 1 explains the lettering. The cooling system consisted of an outer pyrex glass dewar (I), which was filled with liquid N_2, another pyrex dewar (H), filled with liquid He-4, an "inner" He-4 pot (O), into which He-4 gas was condensed, and a He-3 pot (Q), into which He-3 gas was condensed. The SPA (T) was brought into contact with the outer baths by putting exchange gas in the sample can (N), and into contact with the inner baths by spring loading it onto the cooling platform (U).

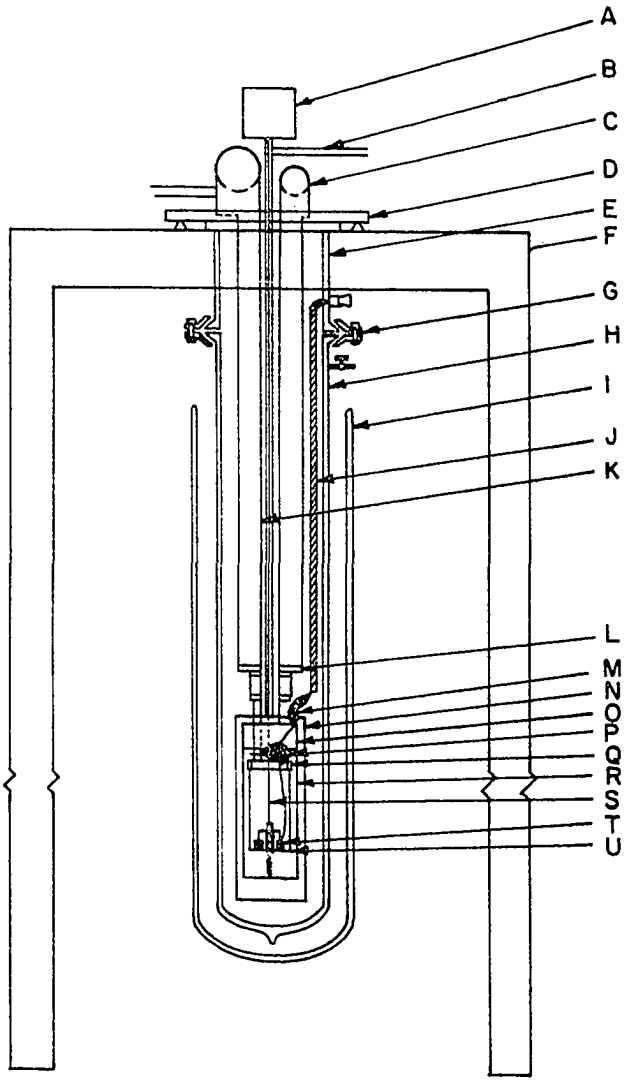

Fig. 2. Schematic view of main body of He-3 calorimeter

Table 1. Explanation of lettering in Fig. 2

Letter	Name and/or description
A	winch
B	sample space pumping line
C	"inner" He-4 pumping line
D	brass plate
E	brass neck
F	wood stand (7' high, 37" wide, 31" deep), mounted on hard rubber pads
G	tapered flange couplers, 4" i.d.
H	He-4 dewar
I	N_2 dewar
J	Al foil, wrapped around fourteen #36 Cu wires
K	He-3 pumping line
L	brass coupler
M	electrical "takeout" (Stupakoff type)
N	sample can
O	He-4 pot
P	terminal panel
Q	He-3 pot
R	shield
S	winch line
T	sample plus addenda
U	cooling platform

The SPA was thermally isolated from the baths by evacuating the sample can, and lifting the SPA off the cooling platform with a winch (A). The "lift off" is commonly referred to as "opening the heat switch". In an actual experiment the sample can was evacuated after the SPA had reached 77°K, and the heat switch was opened at about .4°K.

Heat was introduced into the SPA by passing a d-c current through a Pt-9% W wire heater wrapped non inductively around a heater post on the sample holder. The temperature of the SPA was followed by monitoring the resistance of germanium resistors situated in the sample holder.

Figure 3 is a photograph of the main body of the He-3 calorimeter with the outer dewars removed.

2. He-3 system

A schematic of the complete He-3 system is shown in Fig. 4. The He-3 gas was stored in steel bottles 1 and 2, and the output side of the 1402 KBG pump (i.e. the storage volume contained between valves 10, 11 and 12). When purchased, each 2.5 l. He-3 bottle had been filled with 2 liters of He-3 at STP. The grade of He-3 used was labelled "Low He-4" (of the total He, 99.98% was He-3).

Briefly, He-3 gas was introduced into the He-3 system as follows. Valves 1,2,3,5,6,7,10,15,17,19 and 20 were first closed. Valves 11,12,13 and 14 were then opened. From this valve configuration the He-3 could be pumped back into storage with the special Welch 1402 KBG pump by closing valves 9 and

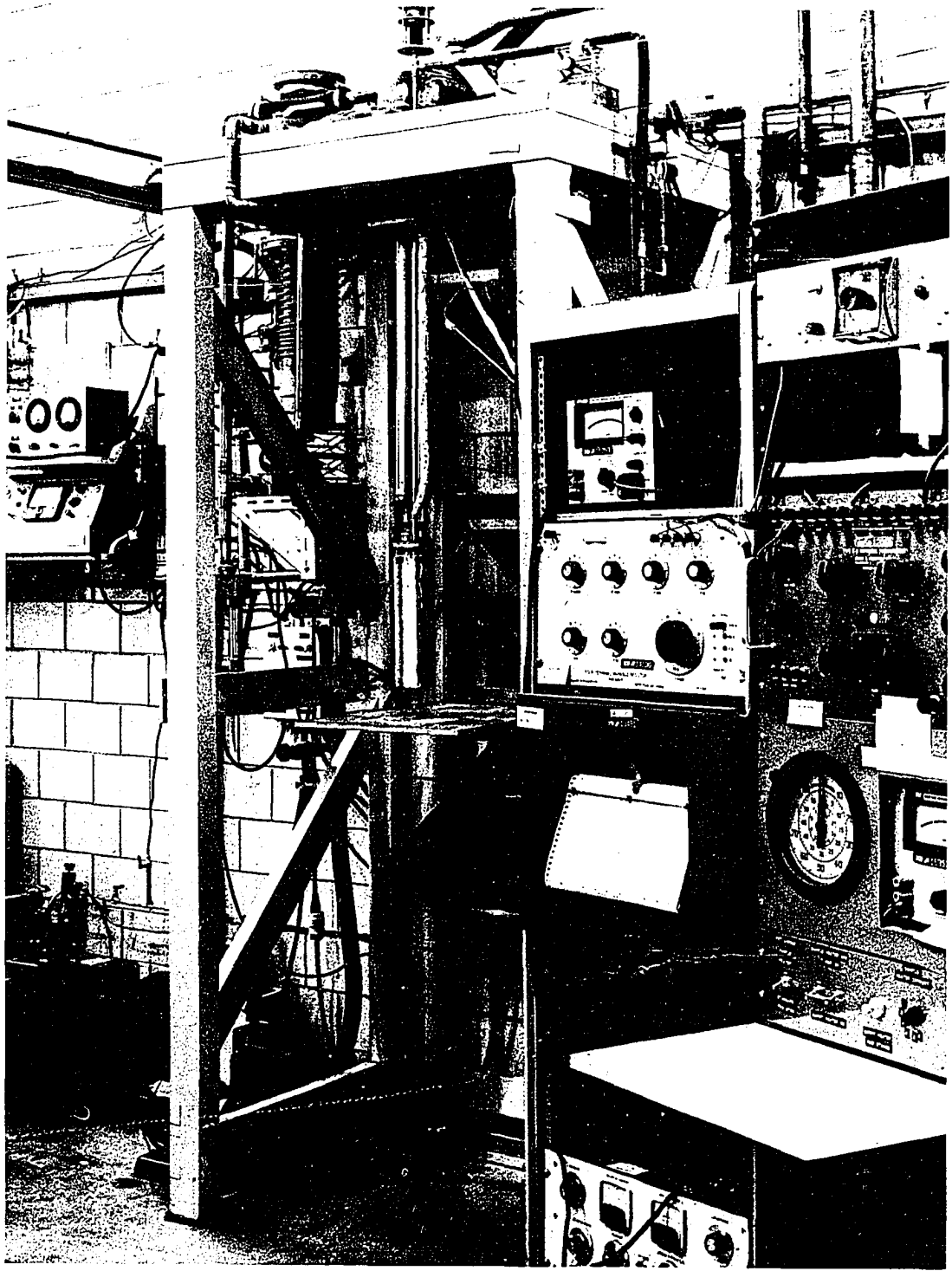

Fig. 3. He-3 calorimeter and associated electronics

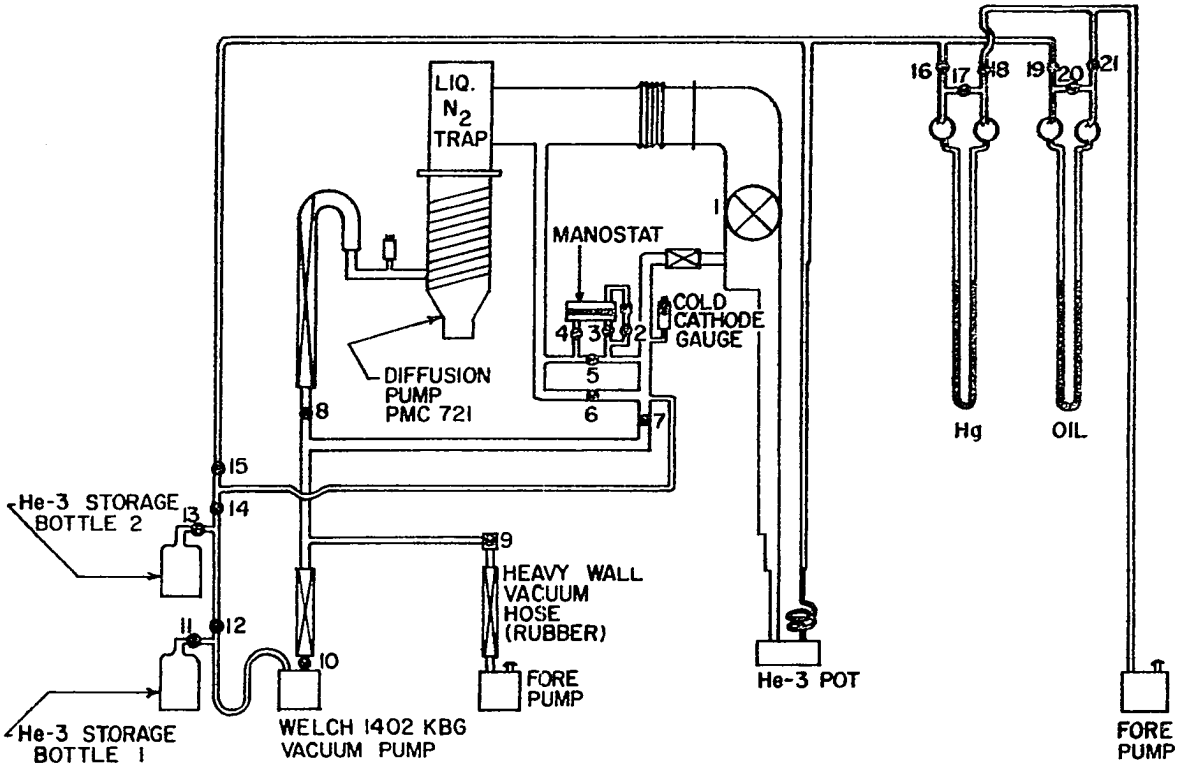

Fig. 4. Schematic view of He-3 system

14, and opening valves 10 and 7, or 10, 6 and 8, or 10, 1 and 8. Further discussion of the He-3 system will be found in sections III A 6 a and sections IV A and B.

3. "Inner" He-4 system

A schematic of the "inner" He-4 system is shown in Fig. 5. The molecular sieve (Linde 5A) trap was placed in liquid N_2 to remove water vapor and air impurities from the bottled He-4 gas. The flow gauge was a differential pressure Hg manometer gauge, which was calibrated by measuring the amount of water displaced from a graduated cylinder within a given time versus the Hg level readings. From such measurements a table of cm^3 He-4/sec vs. manometer reading was prepared (Ames Lab notebook KI-1 p. 195). Further discussion of the inner He-4 system will be found in sections III A 6 a, and IV A and B.

4. Sample space system

A schematic of the sample space system is shown in Fig. 6. The Cu flex tubing was anchored to the wood stand (F, Fig. 2) with lead weights to prevent pump vibrations from traveling down the sample space line to the sample holder. Such vibrations add extraneous heat to the sample holder plus sample, which is undesirable because it is random in time, and also because it raises the lowest temperature attained by the sample. Exchange gas was admitted to the sample space system through valve 1. Further discussion of the sample space can be found in sections III A 6 a and sections IV A and B.

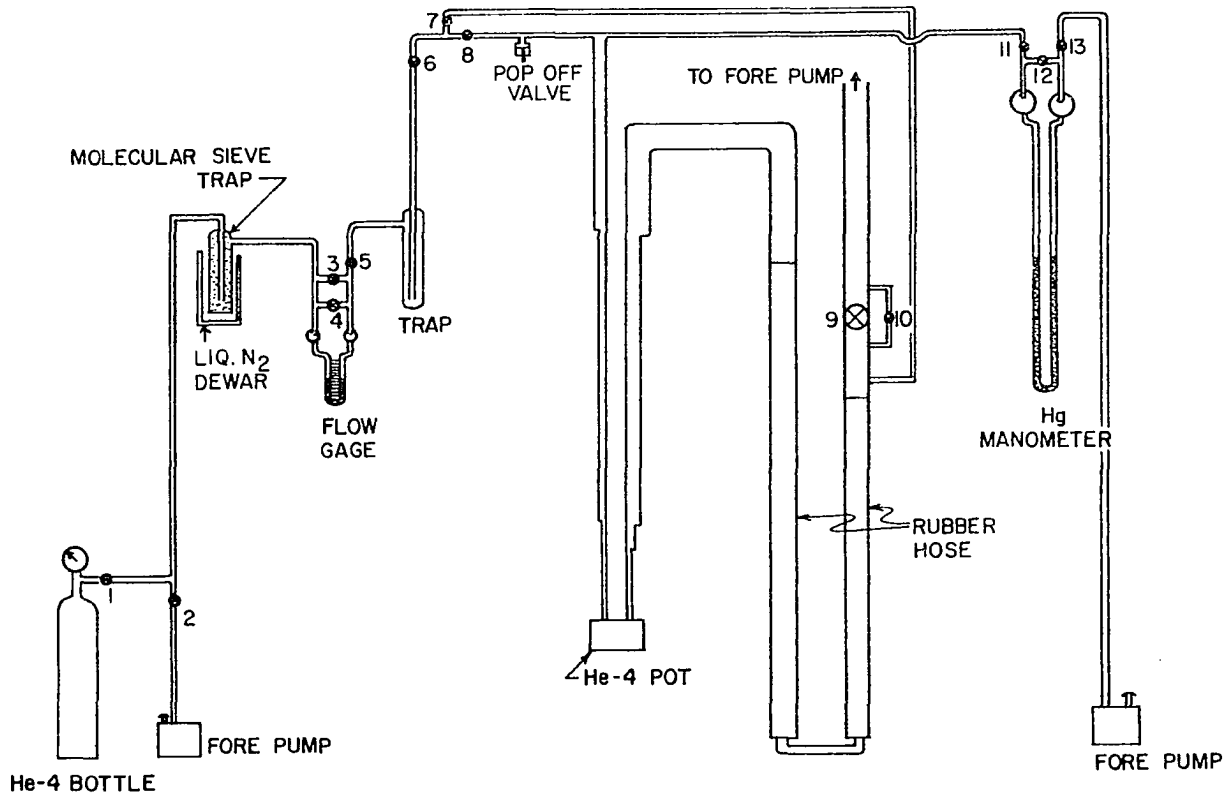

Fig. 5. Schematic view of "inner" He-4 system

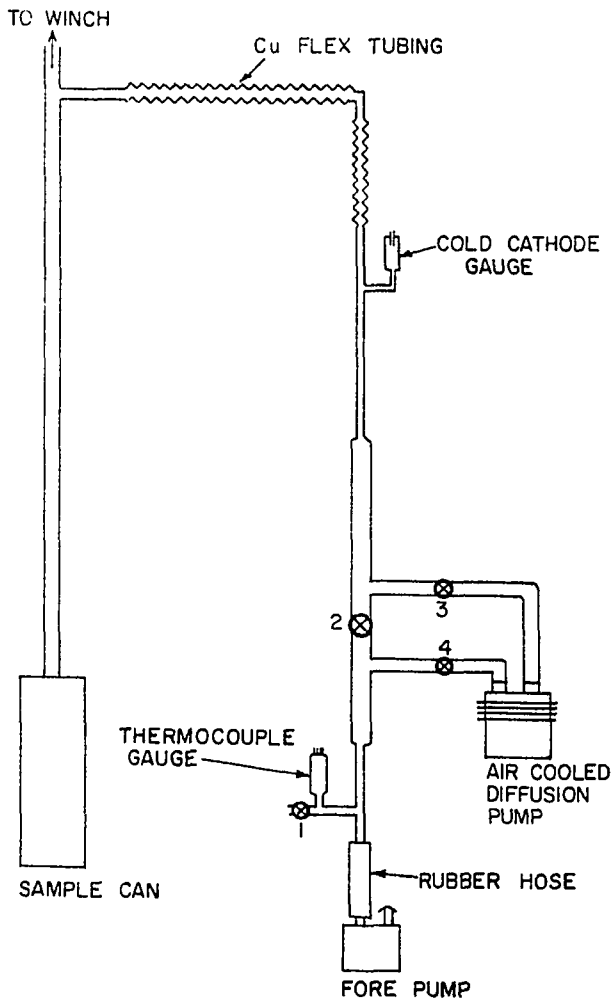

Fig. 6. Schematic view of sample space system

5. Winch system

A schematic diagram of the winch system is shown in Fig. 7. The lower end of the stainless capillary line (30 mil o.d., 8 mil i.d.) was thermally anchored to the outer He-4 bath by two Cu wires (#30, B&S gauge), as shown in Fig. 7. Only one wire is shown. Further discussion of the winch system can be found in sections III A 6 a and section IV B.

6. Detailed description of low temperature section

The low temperature section is taken to be that part of the apparatus below the brass plate (D, Fig. 2). The dewars (H) and (I) will be omitted from this discussion. For purposes of description the low temperature section will be divided into two parts, labelled "lower" and "upper" sections.

a. Lower section A cross-sectional view of the lower section of the low temperature section is shown in Fig. 8, and photographs showing the lower section in several stages of assembly before a measurement are given in Figs. 9, 10, and 11. For the sake of clarity the thermometer and heater leads seen in the photographs are omitted from Fig. 8. The materials of construction and pertinent dimensions are summarized in Table 2.

1). Sample can The sample can consisted of two parts. The upper part (U) was permanently fixed in position by hard soldering to the He-3 pumping line (W) and to the He-4 pumping line (E). The lower part (G) was attached to the

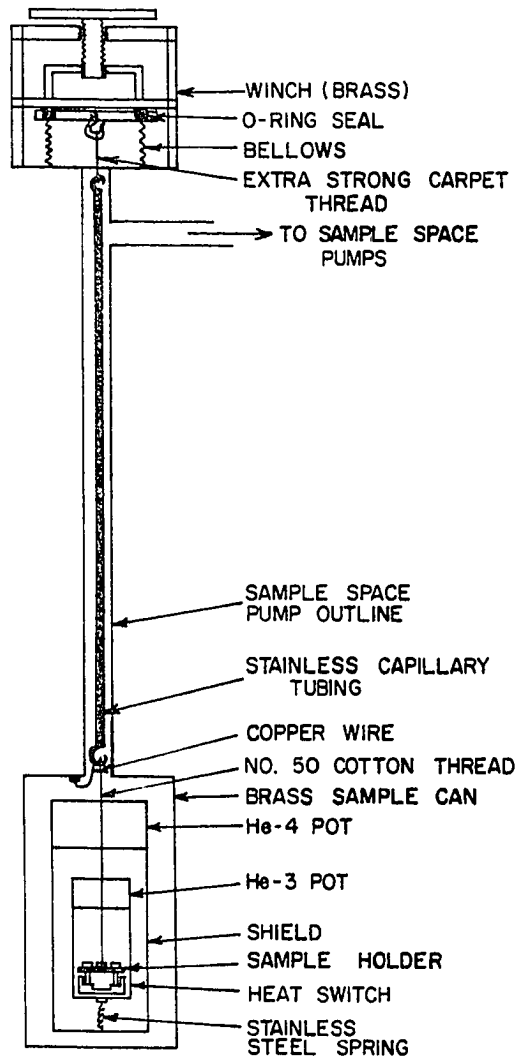

Fig. 7. Schematic view of winch system

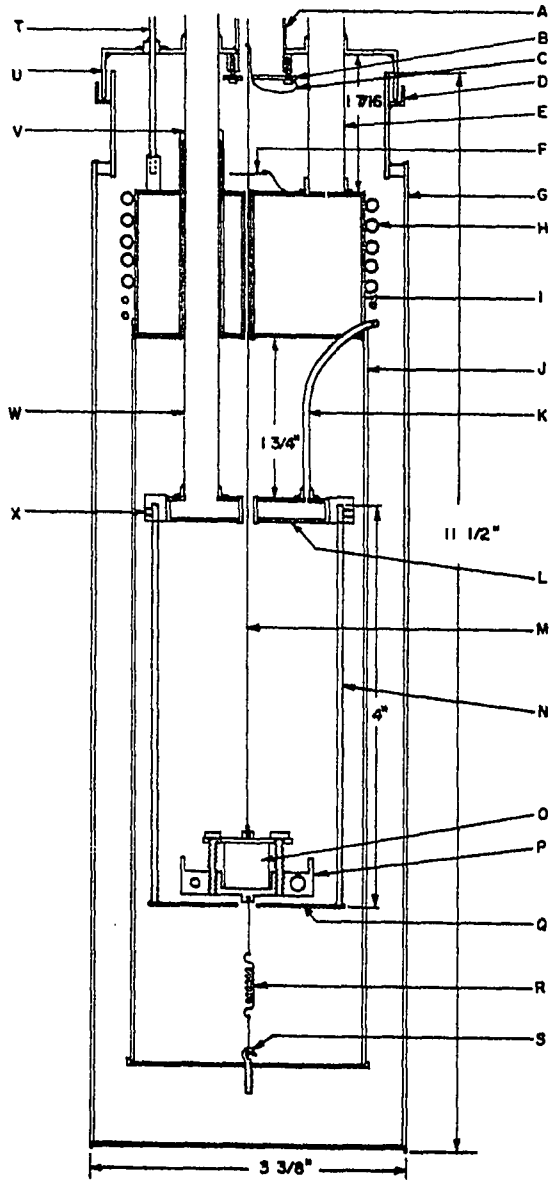

Fig. 8. Cross sectional view of lower part of "low temperature section" of He-3 calorimeter

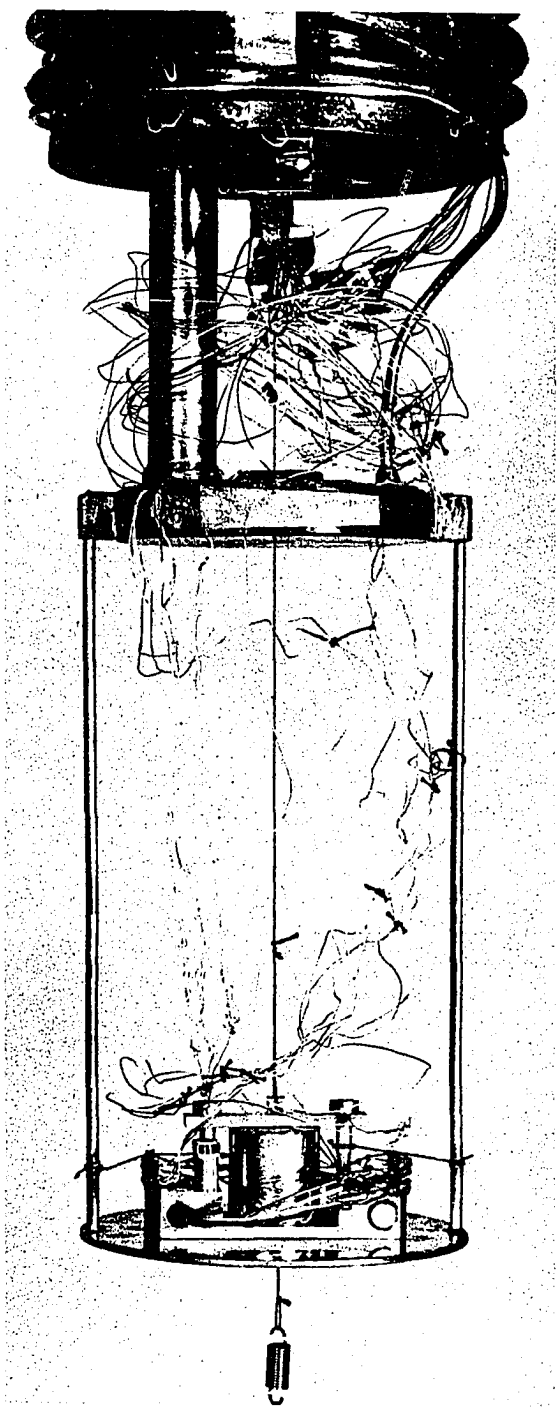

Fig. 9. Lower part of "low temperature section" of He-3 calorimeter, with shield removed

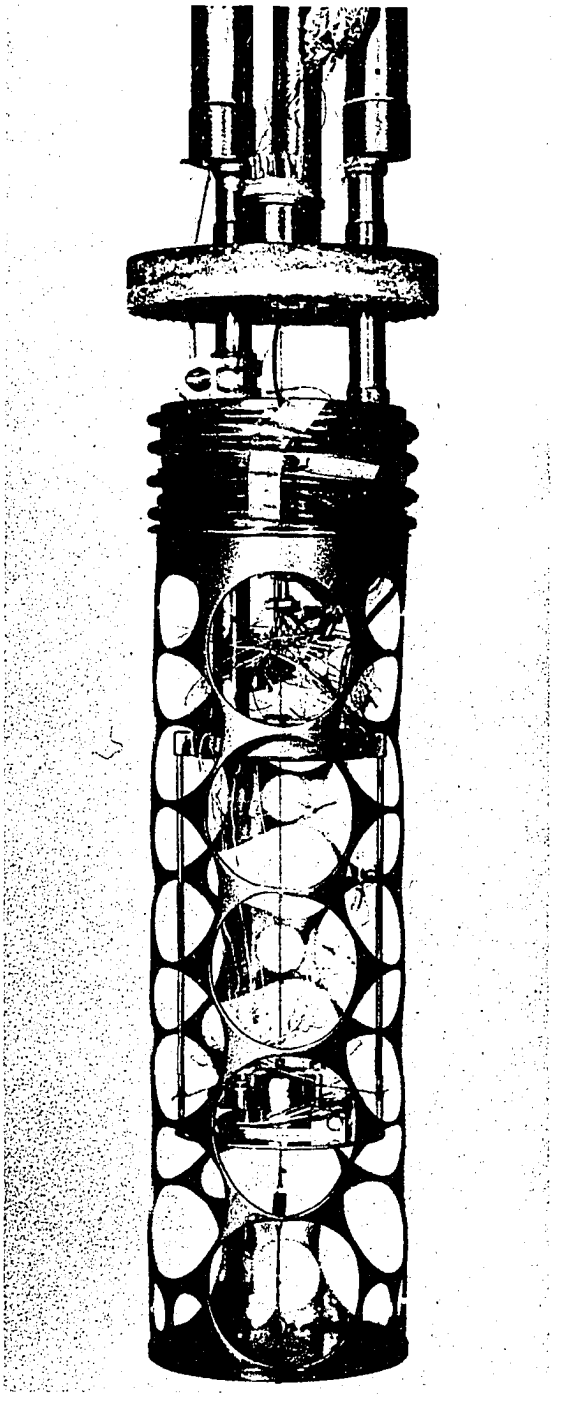

Fig. 10. Lower part of "low temperature section" of He-3 calorimeter, with part of shield added

Fig. 11. Lower part of "low temperature section" of He-3 calorimeter, with shield in place

Table 2. Explanation of lettering, materials of construction, and dimensions of items in Fig. 8

Letter	Description and/or materials of construction	Pertinent dimensions
A	Sample space pumping line, stainless steel	1/2" o.d., 10 mil walls
B	Radiation shield, copper	2 15/32" o.d., 1/32" walls, 8" height
C	Winch line thermal anchor, hard soldered to winch line	5" of #30 Cu wire
D	Solder trough, brass	3/16" deep, 1/8" wide
E	He-4 pump-out line, stainless steel	3/8" o.d., 6 mil walls
F	Radiation shield, copper foil, circular, thermally grounded to He-4 pot by 2" of #26 Cu wire	2 mil foil, 1/2" dia.
G	Sample can, lower section, brass	1/32" walls, 11 1/2" height, 3 3/8" o.d. except for 1" section at top having 3" o.d.
H	He-4 input line, soft copper tubing	1/8" o.d., 1/16" i.d.
I	He-4 pot, copper right circular cylinder	1/32" walls, 2 9/16" o.d., 1 1/2" inside height
J	Radiation shield, copper right circular cylinder	1/32" walls, 2 15/32" o.d., 8" height
K	He-3 input line, stainless steel	1/16" o.d., 6 mil walls

Table 2. (Continued)

Letter	Description and/or materials of construction	Pertinent dimensions
L	He-3 pot, copper right circular cylinder	1/32" walls, 1 7/8" o.d., 1/4" height
M	Winch line, cotton thread	9" (see Fig. 7), size #50
N	Cu rods	1/16" dia., 4" length
O	Sample (ReO_3), right circular cylinder, wrapped in Cu foil	1/2" dia., 1/2" height
P	Sample holder, OFHC copper	See Fig. 12
Q	Cooling platform, copper (gold plated)	1/32" thick, 2 1/8" dia., 7/32" hole in center
R	Spring, steel	1/8" dia., 5/16" length, made from 20-25 mil wire
S S	Threaded eylet, copper	1/2" length, 2-56 thread
T	He-3 input line	1/16" o.d., 6 mil walls
U	Sample can, upper section, brass	1/32" walls, 3 1/4" o.d., 1/2" height
V	Solder joint, soft solder	
W	He-3 pump-out line, stainless steel	3/8" o.d., 6 mil walls
X	Set screws, copper	3/32" length, 4-40 thread

upper part by filling the trough (D) with Woods Metal solder. Attaching and detaching (G) was easily accomplished by wrapping insulated heating tape around (G) near the trough and melting the solder by controlling the current through the tape with a rheostat.

The space enclosed by the sample can is referred to as the "sample space".

2). He-4 pot The He-4 pot (I) was a right circular cylinder having an effective inner volume of 115 ± 1 cm^3. As can be seen in Fig. 8, two sections of tubing pass through the He-4 pot. One allows the He-3 pumping line (W) to be taken through the pot, and the other allows the winch line (M) to pass through the pot. It should be noted that the 3/8" He-3 line only contacts the He-4 pot at the solder joint (V), 5/8" above the top of the He-4 pot. This feature provides a maximum feasible thermal conduction path between the He-3 and He-4 pots, thus yielding a minimum heat leak from the He-4 pot to the He-3 pot. The lower the heat leak into the He-3 pot, the lower the temperature one can reach by pumping on the He-3, since the He-3 evaporation rate will be lower.

Two lines also enter the He-4 pot. The larger one (E) was 3/8" o.d. stainless steel, 6 mil wall thickness. The smaller line (not shown in Fig. 8 because it was directly behind (E)) was 1/16" o.d. stainless, 6 mil wall thickness. As shown in Fig. 8, line (E) was reduced to a 30 mil orifice

as it entered the He-4 pot to reduce problems with superfluid He-4 during pumping.

3). Shield The shield (J) is best seen in Figs. 10 and 11. Basically, the shield cut down the radiation from the sample can walls to the sample, and served as an anchor for the spring (R) in the winch line. The shield consisted of two main pieces, namely a bottom and a side piece. The latter was in the shape of a right circular cylinder, 8" in length, and $2\frac{1}{2}$" o.d. The side walls were 1/32" thick, and contained random sized holes (as can be seen in Fig. 10) to remove as much mass as possible yet allow the structure to be rigid. The bottom piece was made as follows. A solid piece of 1/32" thick Cu was machined to 2 7/8" diameter. Its edges were then turned up so that it slip fitted into position at the bottom of the side piece (Apiezon T grease was used in the slip joint to enhance thermal contact between the sides and the bottom). A 2-56 hole was threaded into the center of the bottom piece for the threaded eyelet (S). The eyelet served as the anchor point from which the sample holder was spring loaded onto the cooling platform (Q).

The shield slip fitted into position around the bottom of the He-4 pot. Apiezon T grease was again used in the slip joint. There was also a screw-type clamp arrangement, similar to that on a hose clamp, at the top of the shield which allowed the shield to be squeezed snugly onto the He-4 pot.

The shield was wrapped with Al foil, to provide a thin, low emissivity surface around the sample, as shown in Fig. 11. Six turns of #26 Cu wire were wound around the Al foil in a helix fashion. One end of the Cu wire was clamped to the He-4 pot (I) with a hose clamp just below (V). The other end of the wire was clamped between two hex nuts that were screwed onto the eyelet (S). This arrangement was found necessary to bring the shield, especially the eyelet, to the He-4 pot temperature, and thus to reduce the heat leak from the eyelet to the sample holder to a minimum.

4). He-3 pot The He-3 pot is shown in Fig. 8 as (L), and also in Fig. 9. It was a right circular cylinder having an effective volume of $5.8 \pm .3$ cm^3. Circular grooves, about .030" wide and 1/16" deep, were machined into the inside bottom of the pot to increase the surface area contact between the pot and the liquid He-3.

Two lines entered the He-3 pot. One (W) was 3/8" o.d. stainless steel, with 6 mil wall thickness, and the other (K) was 1/16" o.d. stainless with 6 mil walls. The smaller line was intended as the input line for the He-3 and the larger line was intended as the pump-out line. Eventually the larger line was used for both purposes.

5). Heat switch The heat switch consisted of two Cu rods (N) hard soldered to a circular Cu plate (Q), commonly called the cooling platform. The plate had a 7/32"

hole in the center to allow attachment of the spring loading line to the sample holder. To improve the thermal contact between the cooling platform and the sample holder, the platform was gold plated (with ~ a 4 mil layer on both sides), and polished with a buffing wheel and red jewelers rouge. The heat switch was attached to the He-3 pot, as shown in Fig. 8, by inserting the rods into snugly fitting holes in the He-3 pot and tightening the set screws located in the sides of the holes. Apiezon T grease was dabbed on the ends of the rods and on the set screws to enhance thermal contact.

6). Sample holder The sample holder is shown as (P) in Fig. 8. A more detailed drawing is shown in Fig. 12. It was made entirely from OFHC (oxygen free, high conductivity) copper. It was polished and gold plated before use. Before polishing and gold plating it weighed 20.4013 g. After gold plating and repolishing it weighed 20.4065 g. As shown in Figs. 8 and 12, the sample holder had two thermometer wells. One was 5/32" diameter, and housed the "high temperature" thermometer (Ge 603). The other was 1/8" in diameter, and housed the "low temperature" thermometer (Ge 311).

The heater post (on the sample holder) was made as follows. A rod (1/2" length, 1/8" dia.) was machined from OFHC Cu. It was deliberately made about .003" oversized for the hole that had been drilled for it in the sample holder, and was shrunk to fit the hole by immersing it in liquid N_2.

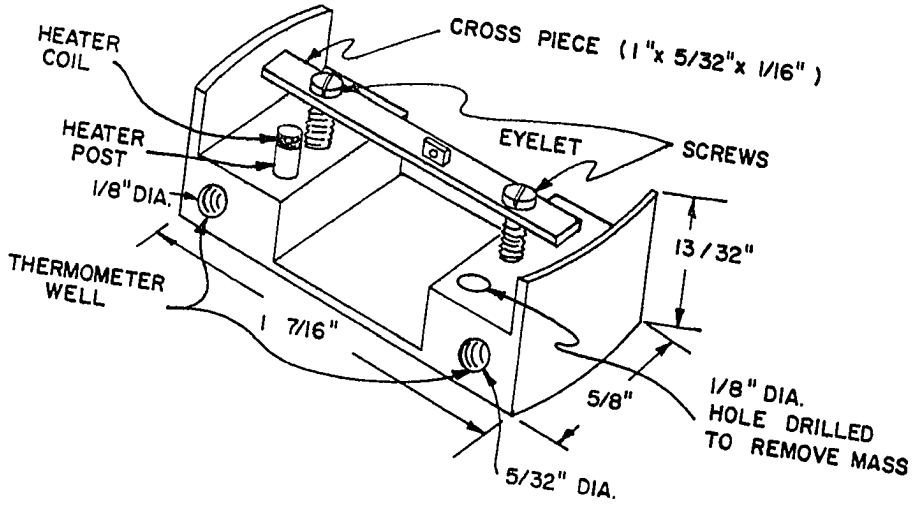

Fig. 12. Oblique view of sample holder

After the rod was shrunk and inserted into the sample holder, it warmed and expanded to fit very tightly into the sample holder.

As can be seen in Fig. 9, the sample holder was tied to the cooling platform rods with two pieces of #50 cotton thread. The length of the thread was such that it was pulled taut when the sample holder was lifted about 1/8" off the cooling platform, at room temperature. This thread arrangement was included to prevent excessive heating of the sample holder due to vibrations after it had been lifted off the cooling platform.

7). Terminal panel The terminal panel (P, Fig. 2) was located between the He-3 and He-4 pots. It can be seen in Fig. 9 directly under the screw in the bottom of the He-4 pot. Below the terminal panel 3 mil manganin was used for most of the leads in order to minimize the heat leak down the leads to the He-3 pot and to the sample holder, while above the panel #36 Cu wire was used.

The terminal panel consisted of 14 pieces (each 1/4" in length) of #20 Cu wire hanging from, and epoxied into, a strip of vector board (2 1/4" x 1/4" x 1/32"). Each piece of Cu (shaped like a J) served as a terminal. The vector board strip was suspended at each end from the He-4 pot, using two pieces of #20 Cu wire. These two pieces of Cu wire (each ~1/2" long) were epoxied to the vector board, and fastened

to the He-4 pot with a screw arrangement like that used to suspend the heat switch from the He-3 pot (see Fig. 8).

Fourteen #36 Cu wires (Q formex insulation) each ~ 20" in length, were taken in a bundle from the fourteen terminals to the electrical takeout (M, Fig. 2). The bundle was wrapped several times around the He-4 pot, and glued to it with GE 7031, for thermal anchoring.

8). Heater The heater can be seen wrapped around the top of the heater post in Fig. 12. It had a room temperature resistance of 1152 ± 3 ohms, and a helium temperature resistance of 1073 ± 1 ohms. A schematic of the heater circuit in the lower part of the low temperature section is shown in Fig. 13.

The heater was made from 34" of 1 mil Pt-9% W wire (Class A enamel insulation) as follows. A layer of onion skin paper was wrapped around a wooden rod having the same diameter as the heater post. The Pt-9% W wire was wound non-inductively (bifilarly) by hand on the onion skin and taped down with masking tape. The coil-and-onion-skin was then slipped off the wooden form, and onto the heater post. GE 7031 varnish was used to glue the onion skin to the heater post, with care being taken not to put any of the GE 7031 on the coil itself, since some insulating materials are known to be dissolved by GE 7031.

About 1/2" from the heater post the two Pt-9% W leads

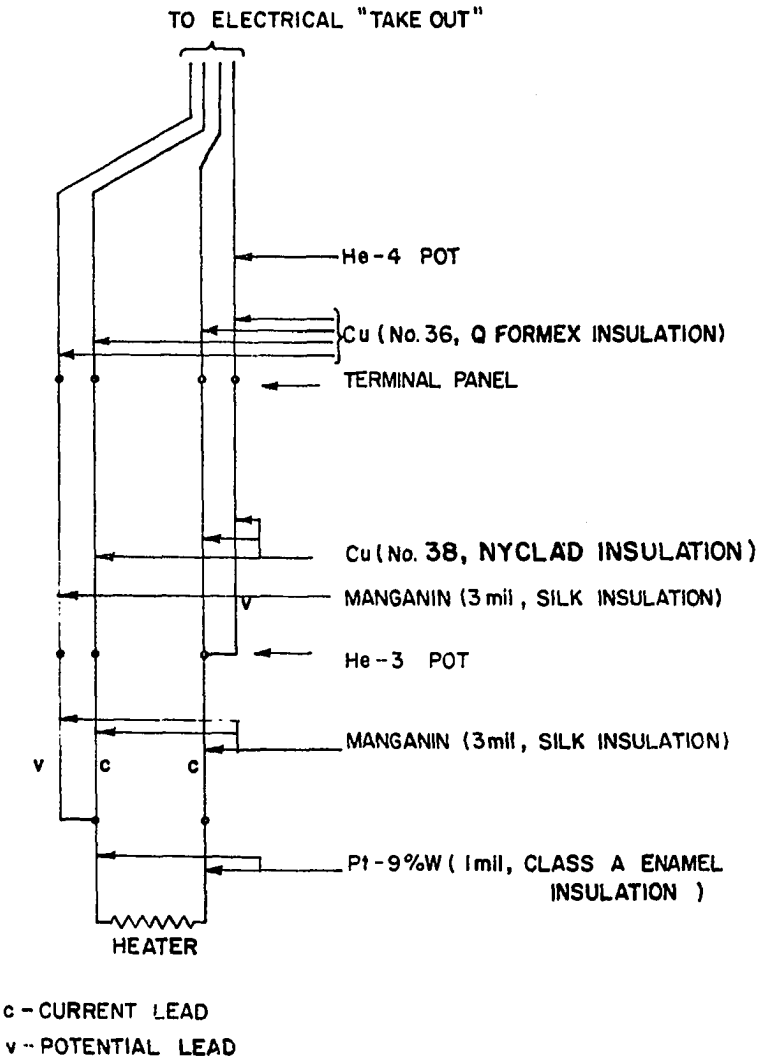

Fig. 13. Schematic view of heater, and associated lead arrangement, within calorimeter sample can

were silver soldered to three 3 mil (silk covered) manganin leads. Two of the manganin leads were connected to one Pt-9% W lead, as shown in Fig. 9. Such a circuit arrangement takes into account the small amount of heat that reaches the sample from Joule heating in the manganin leads, as explained elsewhere (43).

The manganin leads were taken from the heater post to the He-3 pot, where they were thermally anchored by gluing them to masking tape (with GE 7031), which in turn was taped and glued (with GE 7031) to the side of the He-3 pot. The manganin lead length between the heater post and the He-3 pot was about 3" for each lead.

From the He-3 pot to the terminal panel (P, Fig. 2), the heater leads were made up of three #38 Belden Cu wires (Nyclad insulation), and one 3 mil manganin (silk covered) wire as shown in Fig. 13. These leads were thermally anchored to the He-3 pot by gluing a 1½-2" section to masking tape, and taping and gluing the masking tape to the He-3 pot. GE 7031 was used as the glue. After leaving the He-3 pot the leads were wrapped a couple times around the He-3 pump-out and input lines, as seen in Fig. 9. The lead length between the He-3 pot and the terminal panel was ~11" for each lead.

From the terminal panel to the electrical "takeout" (M, Fig. 2), the heater leads were #36 Cu wire (Q formex insulation) as previously described under Terminal Panel.

9). Thermometers Two doped Ge resistors labelled as Ge 603 and Ge 311 were used as thermometers. Ge 603 was calibrated from ~1-28°K, and Ge 311 was calibrated from ~.45-2°K, as will be explained later. Ge thermometry has been discussed at length in the literature (44), and a typical Ge thermometer assembly is shown in Fig. 14. A schematic of the thermometer circuit in the lower part of the low temperature section is given in Fig. 15.

a). Ge 603 The thermometer labelled Ge 603 was made by Honeywell Corporation. At 4.197°K it had a resistance of 1040.2 ohms. Its outer case was 9/16" in length, and .137" in diameter. The outer case was coated with Apiezon T grease before it was placed into the 5/32" thermometer well (Fig. 12). When purchased, Ge 603 had four 10" leads. Two were current, and two were potential leads. Each was covered with spaghetti insulation. These leads were shortened to 1½" for use in the calorimeter. Each lead was made up of 6 strands of tinned Cu wire. After the 1½" of tinned Cu, 3 mil manganin wire (silk covered) was used for the thermometer leads, up to the terminal panel (P, Fig. 2). Low thermal solder was used to make all solder joints in the thermometer leads.

About 1 3/4" - 2" away from the thermometer case a section (~½" in length) of the manganin leads was thermally anchored to the sample holder as follows. Masking tape was

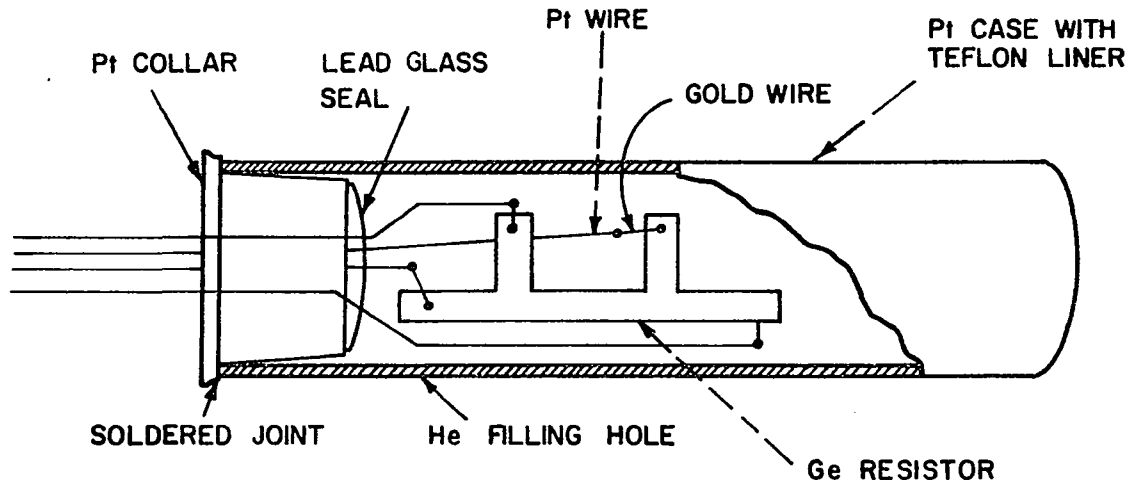

Fig. 14. Typical Ge thermometer assembly

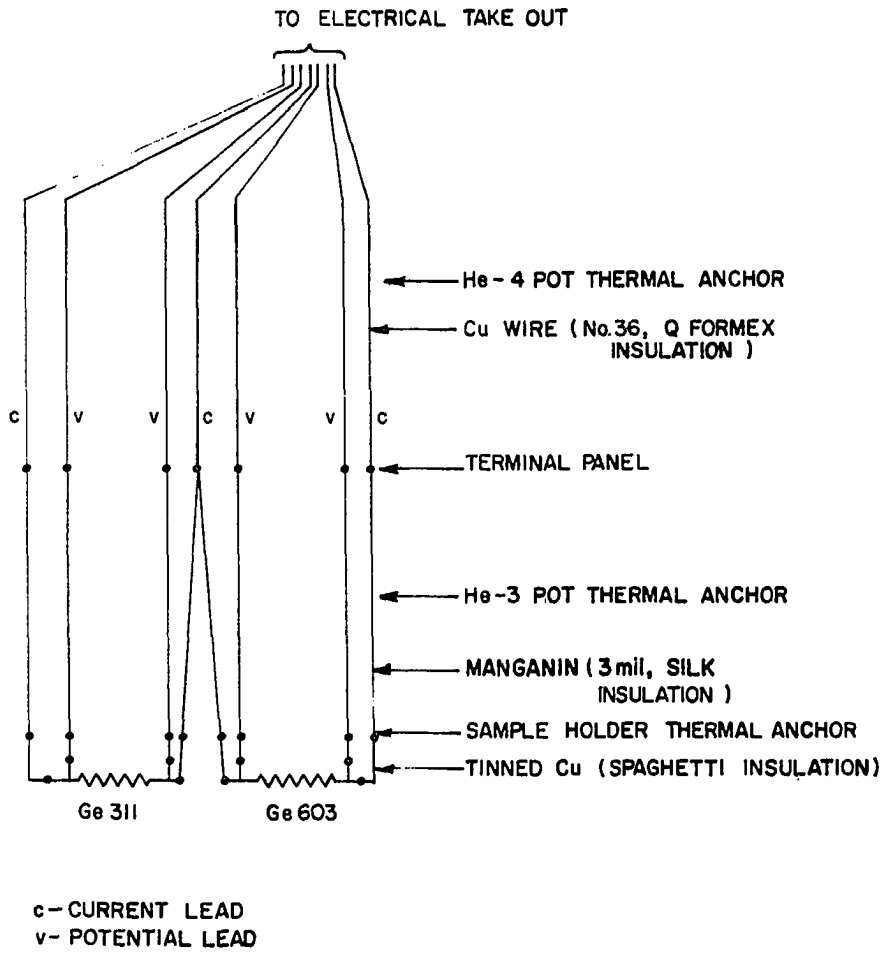

Fig. 15. Schematic view of thermometers, and associated lead arrangement, within calorimeter sample can

glued, with GE 7031, to the sides of the sample holder facing the rods of the cooling platform. The manganin leads were then glued to the masking tape with GE 7031. The anchoring was done to improve thermal contact between the thermometer and the sample holder.

After leaving the sample holder, the manganin thermometer leads were taken to the He-3 pot, where a section (1½" - 2") was thermally anchored in a manner as described in the above paragraph. In this case the anchoring was done to reduce the heat leak down the leads from the He-3 pot to the sample holder. From the He-3 pot to the sample holder each lead was ~11" in length.

After leaving the He-3 pot, the manganin leads were wrapped a couple times around the He-3 pump-out and input lines, and then taken to the terminal panel. Between the He-3 pot and the terminal panel each lead was ~11" in length.

From the terminal panel to the electrical "takeout", the thermometer leads were #36 Cu wire (Q formex insulation) as previously described under Terminal Panel.

b). Ge 311 The Ge thermometer labelled Ge 311 was made by Cryocal Corporation. It had a resistance of ~295 ohms at ~1°K. The outer case was .335" in length and .124" in diameter. It was coated with Apiezon T grease, loaded, and wired in the same way as Ge 603 (described in the previous section).

b. Upper section The "upper" section of the low temperature section is roughly that part of the apparatus from the top of the sample can (N, Fig. 2) to the brass plate (D, Fig. 2). A schematic cross sectional view of the "upper" section is shown in Fig. 16. An explanation of the labels, dimensions, and materials of construction are given in Table 3.

7. Thermometer circuit

Ge thermometer resistance was measured using a Guildline Instruments "isolating potential comparator" (ISOPOCO), a Guidline variable standard resistor (VASTAR), model 9801-T, a Fluke 845AB null detector, and a Honeywell Electronik-15 chart recorder. The general technique of resistance measurement using ISOPOCO was originally suggested by Dauphinee (45), and can be explained with the simplified thermometer circuit shown in Fig. 17.

When VASTAR is set at exactly the resistance of the Ge thermometer, the voltage drop across the thermometer, V_T, will equal the voltage drop across VASTAR, V_S, since the current is the same through both. As can be seen in Fig. 16, the voltage drop across the thermometer is used to charge the capacitor, C. The capacitor leads are then "flipped" (with a mechanical chopper) to put the capacitor across VASTAR. At balance, $V_S = V_T$, the capacitor will neither charge nor discharge, and no current will flow in the voltmeter loop, i.e., the voltmeter will give a null reading, which can be read either on

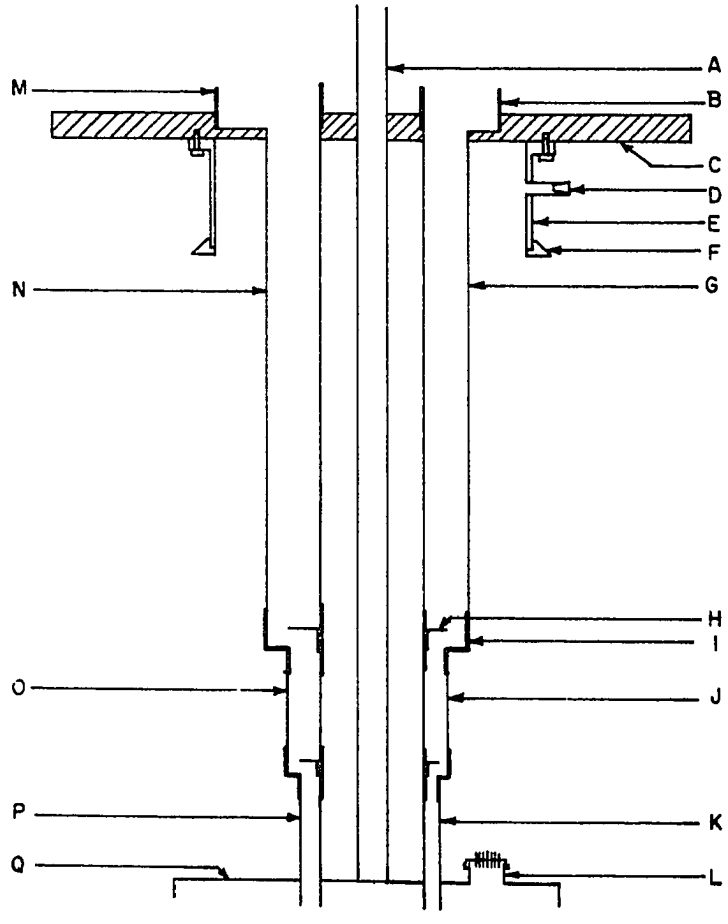

Fig. 16. Schematic cross sectional view of upper part of "low temperature section" of He-3 calorimeter

Table 3. Explanation of lettering, materials of construction and dimensions of lettered items in Fig. 16

Letter	Description and/or materials of construction	Pertinent dimensions
A	Sample space pumping line, stainless steel	1/2" o.d., 10 mil walls, 32 1/4" from C to Q
B	"Inner" He-4 pump out line, copper	2" o.d., 2" length
C	Brass plate	1/2" thick, 14" o.d.
D	Rubber stopper	size - 0
E	Brass neck	4" o.d., 8" length, 1/16" walls
F	Flange, stainless	3 7/8" i.d., 5 3/8" o.d. maximum
G	"Inner" He-4 pump-out line, stainless steel	1" o.d., 20 mil walls, 29" length
H	Radiation trap, brass	5/8" dia., 1/32" thick
I	Coupler, brass	top - 1 1/4" i.d., bottom - 5/8" i.d.
J	"Inner" He-4 pot pump-out line, stainless steel	5/8" o.d., 10 mil walls, 2 1/4" length
K	"Inner" He-4 pot pump-out line, stainless steel	3/8" o.d., 6 mil walls, 1" from coupler to Q
L	Electrical "take out", Stupakoff type, 14 pins	3/4" o.d.

Table 3. (Continued)

Letter	Description and/or materials of construction	Pertinent dimensions
M	He-3 pump-out line, copper	3" o.d., 2" length
N	He-3 pump-out line, stainless steel	1 1/4" o.d., 20 mil walls, 29" length
O	He-3 pump-out line, stainless steel	5/8" o.d., 10 mil walls, 2 1/4" length
P	He-3 pump-out line, stainless steel	3/8" o.d., 6 mil walls, 1" from coupler
Q	Sample can, upper section	see (U), Table 2

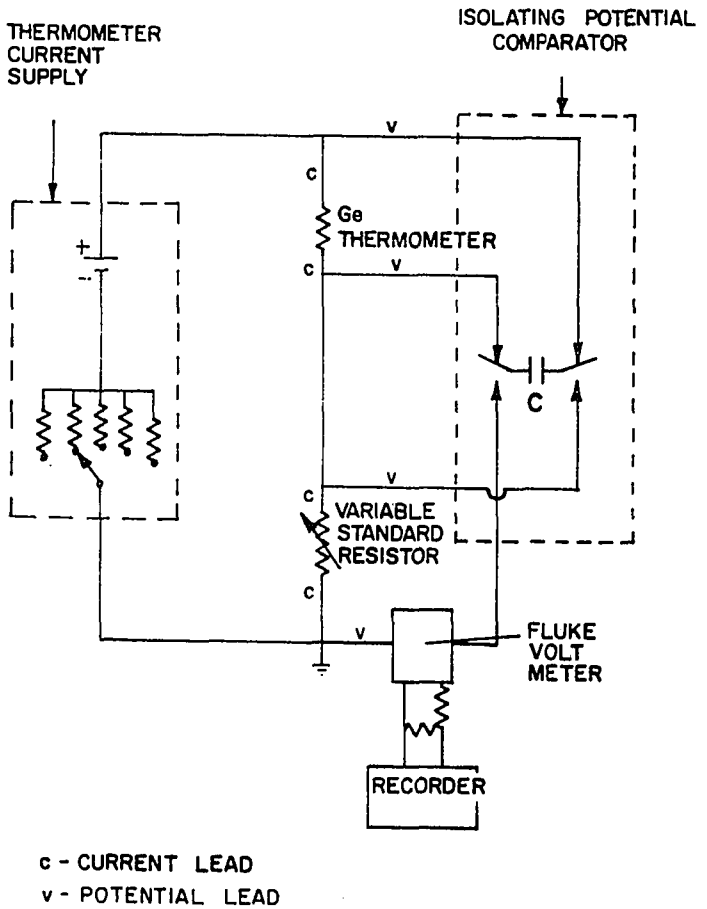

Fig. 17. Simplified thermometer circuit illustrating use of isolating potential comparator

the recorder or the voltmeter. Thus an unknown resistance can be determined by comparing against VASTAR, dialing VASTAR until a null is read on the voltmeter or recorder, and reading the "balance" resistance on VASTAR.

The thermometer circuit used in the He-3 calorimeter was essentially the same as that in Fig. 17, except that a low thermal switch (4 pole, triple throw) was added which put either Ge 603 or Ge 311 in the measuring circuit. A schematic of the thermometer circuit, showing the various components as they were ordered in the panel rack (left rack, Fig. 3) is shown in Fig. 18. From the electrical takeout to the low thermal switch the thermometer leads were #36 Cu wire (Q formex insulation). Each lead was 120" in length.

Shielding of the thermometer leads was carried out as follows. Inside the sample can (N, Fig. 2), the leads were shielded by the can itself, which was grounded by running a lead from earth ground to pumping line (C, Fig. 2). From the sample can (N, Fig. 2) to the rubber stopper "takeout" in the brass neck (E, Fig. 2), the thermometer leads were shielded by Al foil (J, Fig. 2), which was also in contact with the grounded pumping line (C, Fig. 2). From the rubber stopper "takeout" to the low thermal switch (Fig. 17), the leads were shielded with braided shielding cable which was attached (by way of the low thermal switch chassis) to the grounded panel rack (Fig. 17). All the other thermometer leads ex-

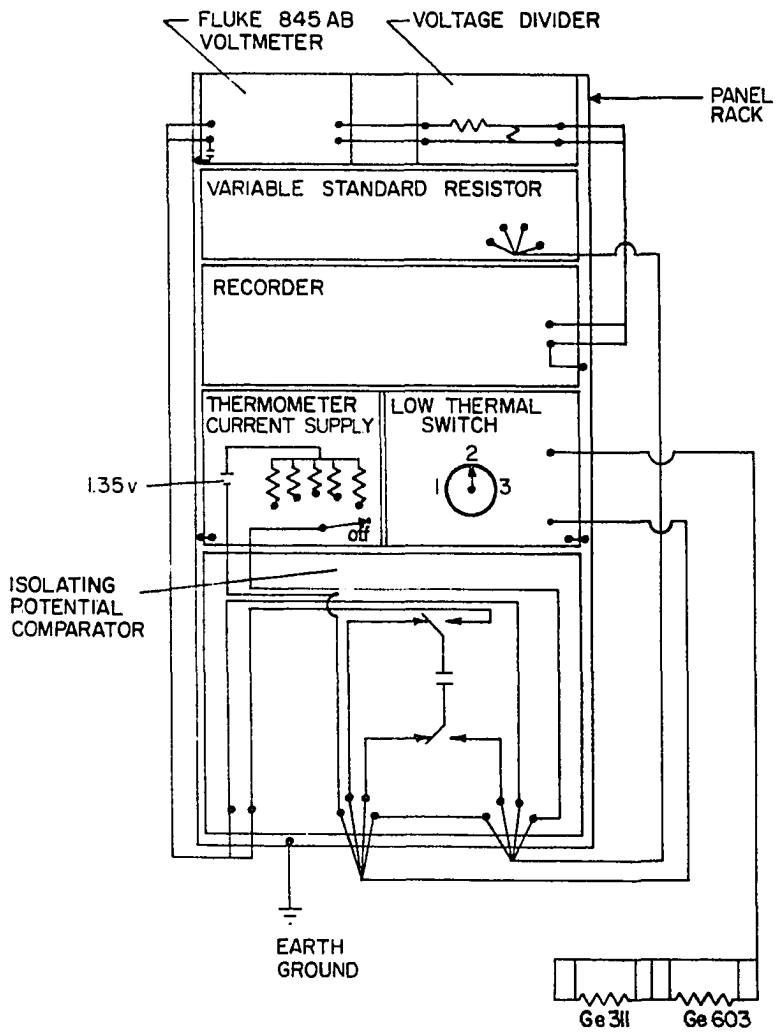

Fig. 18. Schematic diagram of thermometer circuit components for He-3 calorimeter

ternal to the panel rack (see Fig. 18) were two-lead shielded cable with the shielded portion clamped to the grounded panel rack at one point along each cable.

The resistors in the thermometer current supply (Figs. 17 and 18) were such that 10 currents, ranging from ~.1 to ~25 microamps, were available. It was not necessary to measure the thermometer current, nor did it have to be extremely steady with the comparator type of measuring circuit. This is in contrast to standard potentiometric resistance measurements where the opposite is the case.

8. Heater circuit

The lower part of the heater circuit has already been given in Fig. 13. The complete heater circuit is given in Fig. 19. The power supply was made up of two 1.35 volt Hg dry cells in parallel (for greater stability). The selector switch stepped the resistance in the circuit up or down such that heater current could be varied from ~.7 to ~200 microamps in eight steps. The standard resistor was made by Rubicon Co. and had a resistance of 1000.05 ohms. The "dummy" heater was a 0-2 K variable resistor. The potentiometer was a Leeds and Northrup Model K-3, and the null detector was a Fluke model 845 AB voltmeter. The timer-heater switch was made up of two triple pole, double throw switches which were mechanically "ganged" together, such that the heater and timer could be activated "simultaneously" (probably to within

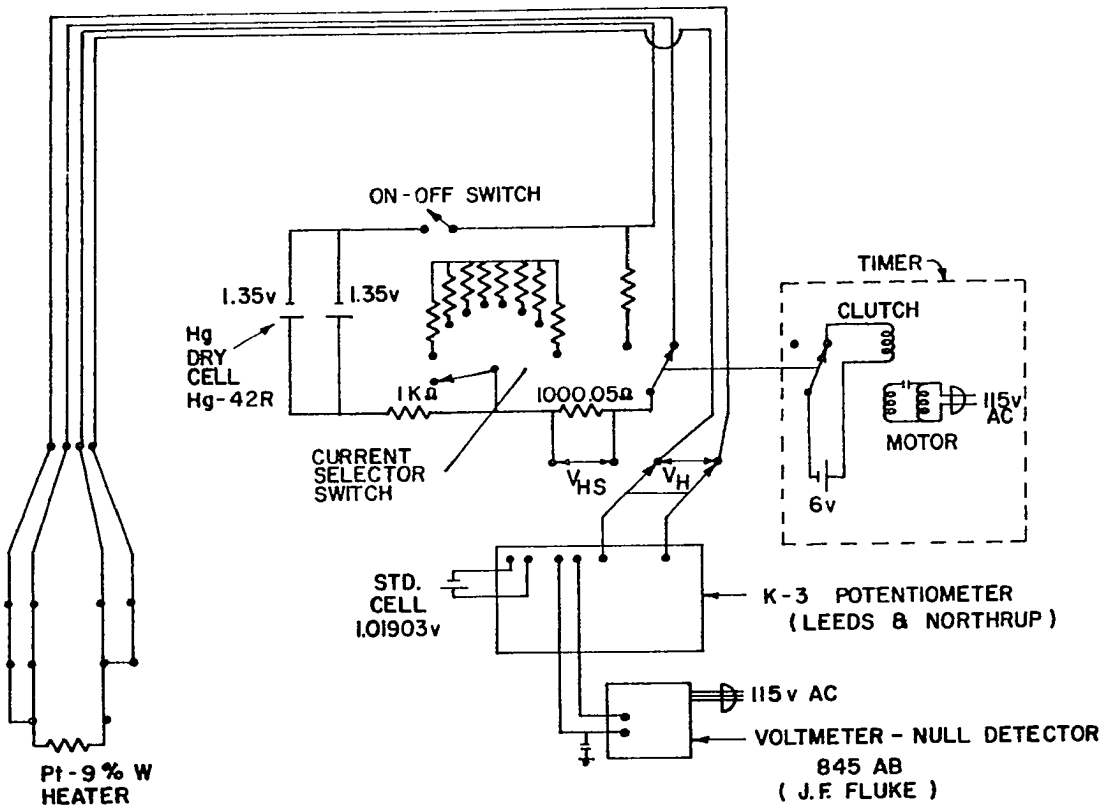

Fig. 19. Schematic diagram of heater circuit of He-3 calorimeter

.02 seconds). The timer, which measured the duration of the heating period, was made by Standard Electric Time Co. (Model No. No. S-13h-10P). It had a 6" diameter dial and could be read to .002 sec.

B. Calibration Apparatus

1. Ge 603

Ge 603 was calibrated from ~1-28°K by comparing it against another Ge thermometer (Gr 618), which belonged to Physics Group II and had been calibrated elsewhere (46). The treatment of the data, and discussion of results are given in section V A and VI A respectively.

The apparatus used for calibration of Ge 603 has also been described elsewhere (46). Briefly, Ge 603 and Gr 618 (along with several others) were placed in a Cu block which could be cooled to ~1°K (using liquid He-4). The block could then be essentially thermally isolated from the cooling bath, and its temperature controlled by a heater-temperature controlling device. While the temperature was held constant (to within ~.002°K), at various temperatures between ~1-28°K, potentiometric resistance readings of the calibrated and uncalibrated thermometers were taken as a function of time.

2. Ge 311 and Ge 312

Germanium thermometer Ge 311 and Ge 312 were calibrated in the range ~.45-2°K using the paramagnetic salt technique. A discussion of the method, treatment of the data and dis-

cussion of the results can be found in sections V A and VI A.

A schematic of the main body of the apparatus used for the calibration from ~.45-2°K is shown in Fig. 20. It can be seen to be a modification of the calorimeter by comparing to Fig. 2. Only those items are lettered in Fig. 20 which are not in Fig. 2. The explanation of the lettering in Fig. 20 is given in Table 4.

Table 4. Explanation of lettering in Fig. 20

Letter	Designation
A	brass to copper to glass (BCG) can
B	copper block
C	copper wires
D	salt pill (CMN)
E	salt pill container
F	mutual inductance coil

A more detailed cross sectional view of the calorimeter modifications made for calibration is shown in Fig. 21, and can be compared with the same cross section of the He-3 calorimeter (Fig. 8). An explanation of the lettering, description of the materials of construction, and dimensions for lettered items in Fig. 21 are given in Table 5. Photographs of the lower part of the calibration apparatus (Fig. 21) at various stages of assembly is shown in Fig. 22.

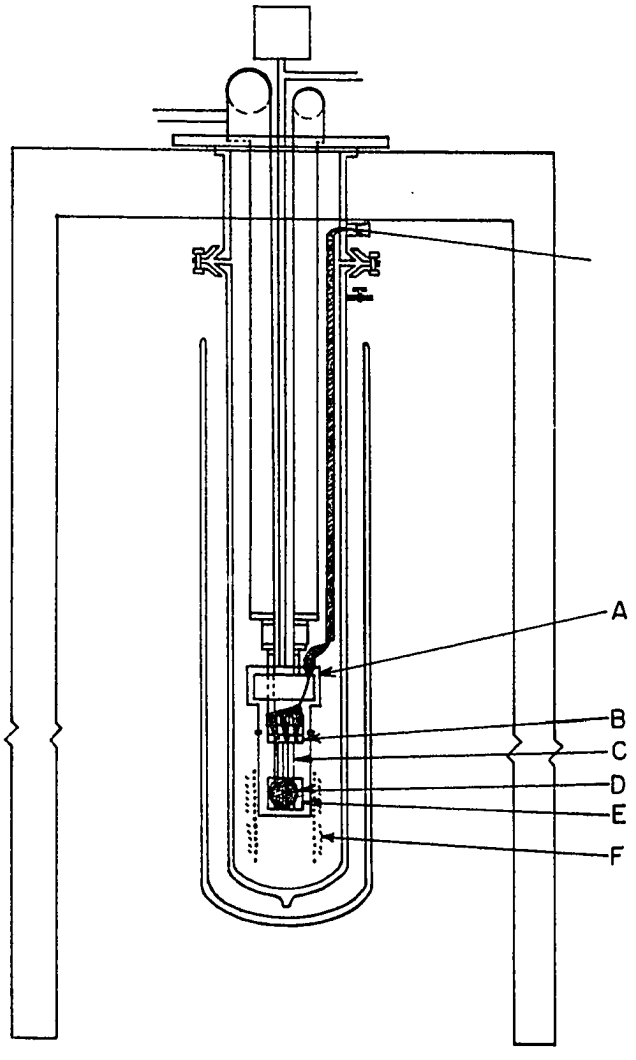

Fig. 20. Schematic view of main body of calibration apparatus

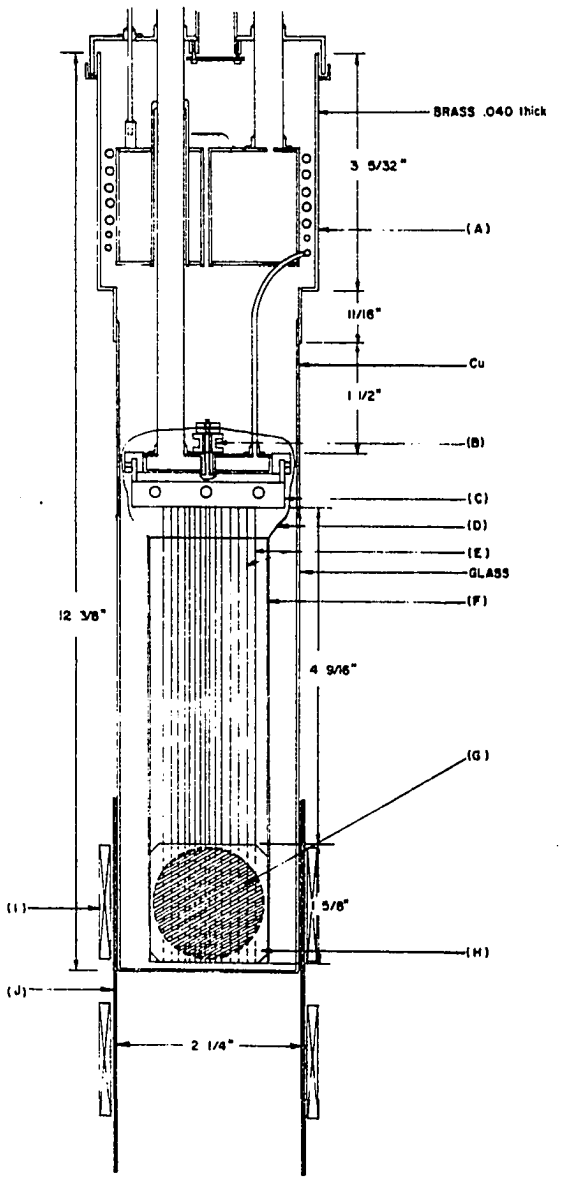

Fig. 21. Cross sectional view of lower part of calibration apparatus

Table 5. Explanation of lettering, materials of construction, and dimensions of lettered items in Fig. 21

Letter	Description and/or materials of construction	Dimensions
A	brass to copper to glass (BCG) can, right circular cylinders	dimensions given in Fig. 21, except (not shown) glass was necked down to 2 1/4" o.d.
B	heater holder, copper	1/2" o.d. maximum, 1/4" o.d. minimum, 3/32" hole 5/16" off center
C	copper block, right circular cylinder	2 1/16" dia., 5/16" height
	3 holes drilled through from sides	middle hole .156" dia., other two .134" dia.
	2 Cu connecting rods hard soldered to Cu block	1/16" dia., 5/16" length
D	Cu wire, thermal anchor from He-3 pot to coil foil	#38 Cu wire
E	Cu wires, seventeen	#26 Cu wire, dimensions shown in Fig. 21
F	"coil foil" radiation shield, made from #38 Cu wires, right circular cylinder	6" length, 1 5/8" i.d.
G	salt pill, sphere, cerous magnesium nitrate powder, $Ce_2Mg_3(NO_3)_{12}\cdot 24\ H_2O$, called CMN	1 1/2" dia.

Table 5. (Continued)

Letter	Description and/or materials of construction	Dimensions
H	salt pill container, right circular cylinder with sphere hollowed out of center, nylon, two halves, plus cap for opening in top (not shown)	1 5/8" dia., 1 5/8" height
I	secondary coil of mutual inductance coil, copper	see Fig. 22
J	primary coil of mutual inductance coil, copper	see Fig. 22

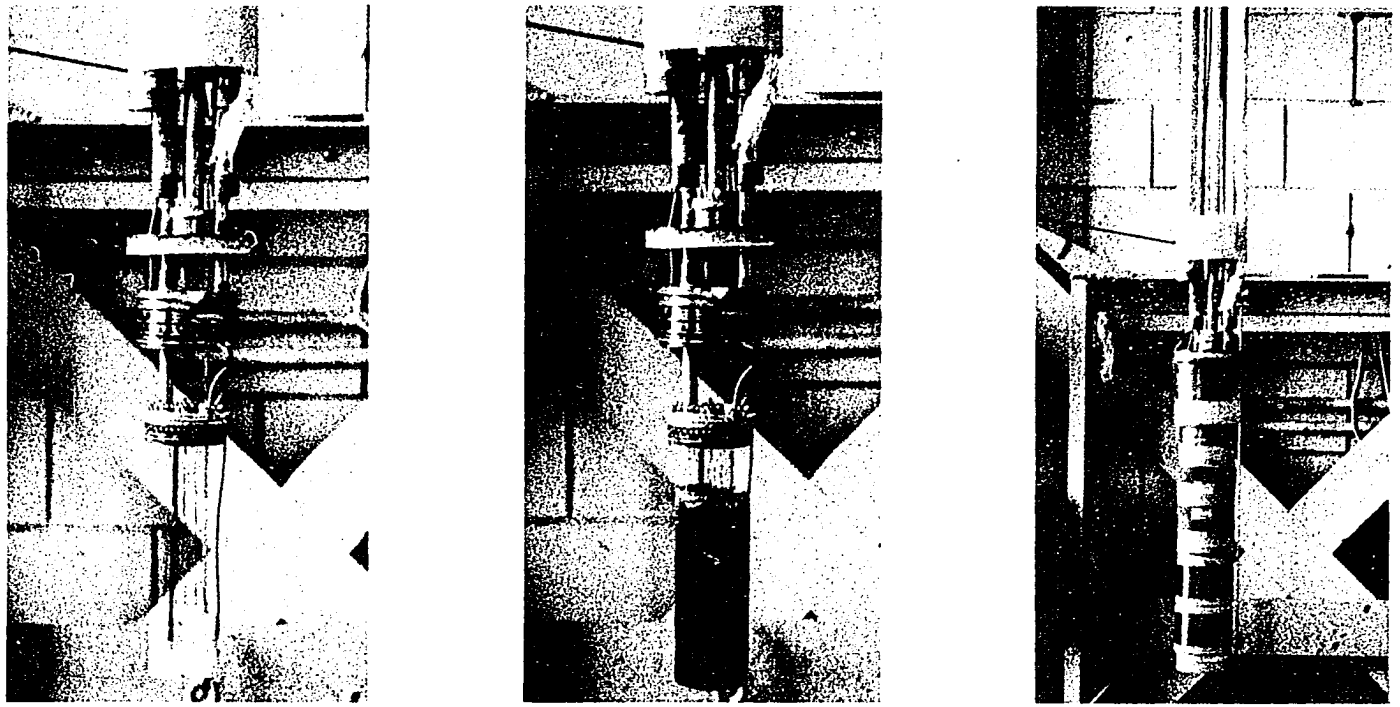

(a) (b) (c)

Fig. 22.. Lower part of calibration apparatus; (a) showing salt pill container, (b) showing coil foil around salt pill container, and (c) with BCG can and mutual inductance coil in place

The calibrated thermometer, Ge 603, and two uncalibrated thermometers Ge 311 and Ge 312 were loaded into thermometer wells in the Cu block, C, which was suspended from the He-3 pot in a fashion like that described under Heat Switch in section III A 6 a. Hanging from the Cu block (C), were 17 #26 Cu wires (E) which passed through the nylon salt pill container (H) and salt pill (E). The Cu wires provided thermal contact between the salt ($Ce_2Mg_3(NO_3)_{12}\cdot 24H_2O$) and the Cu block. The salt pill was surrounded by a "coil foil" radiation shield (F), which was thermally anchored to the He-3 pot by seven #38 Cu wires such as (D). The "coil foil" consisted of ~1000 pieces of #38 Cu wire (each ~6" in length) lying side by side and glued together with GE 7031 to effectively produce a "sheet" of wires, each wire electrically insulated from the other.

The "sheet" was wrapped around the salt pill in such a fashion that each of the 6" lengths of #38 wire was parallel to the wires (E). Thus the salt pill was shielded from radiation from the glass walls, which separated the salt pill from the outer He-4 bath, and at the same time the "coil foil" prevented eddy currents from being generated by the inductance coil (F, Fig. 20), in the radiation shield because there was not a continuous conducting path around the salt pill.

The inductance coil was slipped into position around the bottom of the brass-copper-glass (BCG) can (A, Fig. 21) such

that one section (I), of the secondary was centered on the salt pill (G).

A schematic cross sectional view of the inductance coil is given in Fig. 23. The Cu foil between the primary and the secondary was connected to earth ground to reduce the capacitive coupling between the primary and secondary.

The primary coil contained two layers (525 turns per layer) of #32 Cu wire (heavy polythermaleze insulation), each layer covered with onion skin paper.

The secondary was wound in two sections. In order to make the net mutual inductance between the primary and secondary zero when there was no sample inside the primary the two secondary sections were wound in opposing directions. Each section was made up of 10 layers separated by onion skin paper, using the same kind of wire as for the primary. There were ~1497 $\pm$ 1 turns in each section.

The dimensions of the coil were chosen according to formulae given by Wheatley (47).

The mutual inductance between the primary and secondary was measured using a Hartshorn bridge type of circuit. The bridge circuit is shown in Fig. 24, and has been described elsewhere (48).

The calibration arrangement of the thermometers and associated leads within the BCG can is shown in Fig. 25. Outside the BCG can the thermometer circuit was exactly the same as

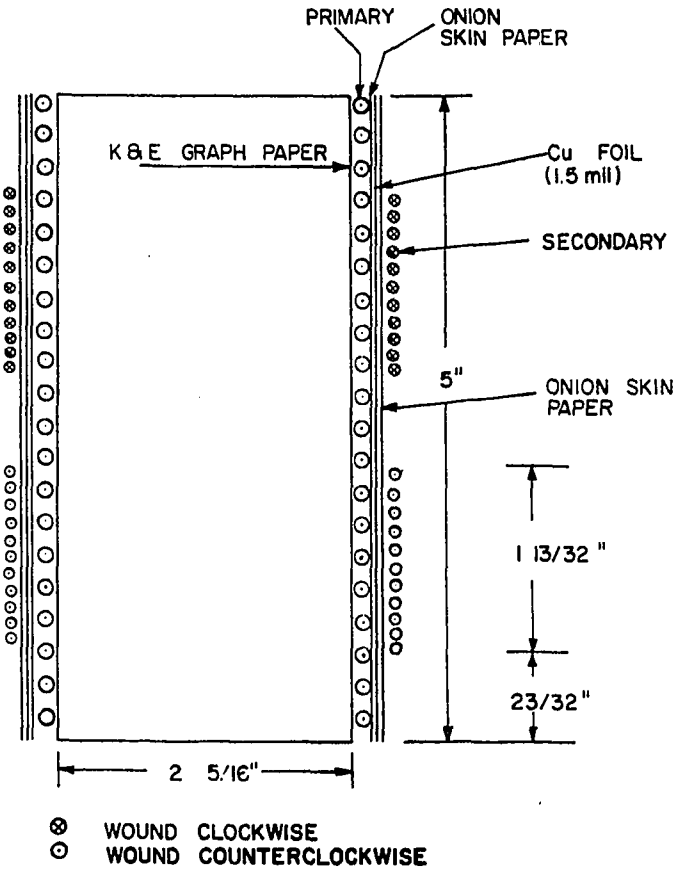

Fig. 23. Schematic cross sectional view of mutual inductance coil

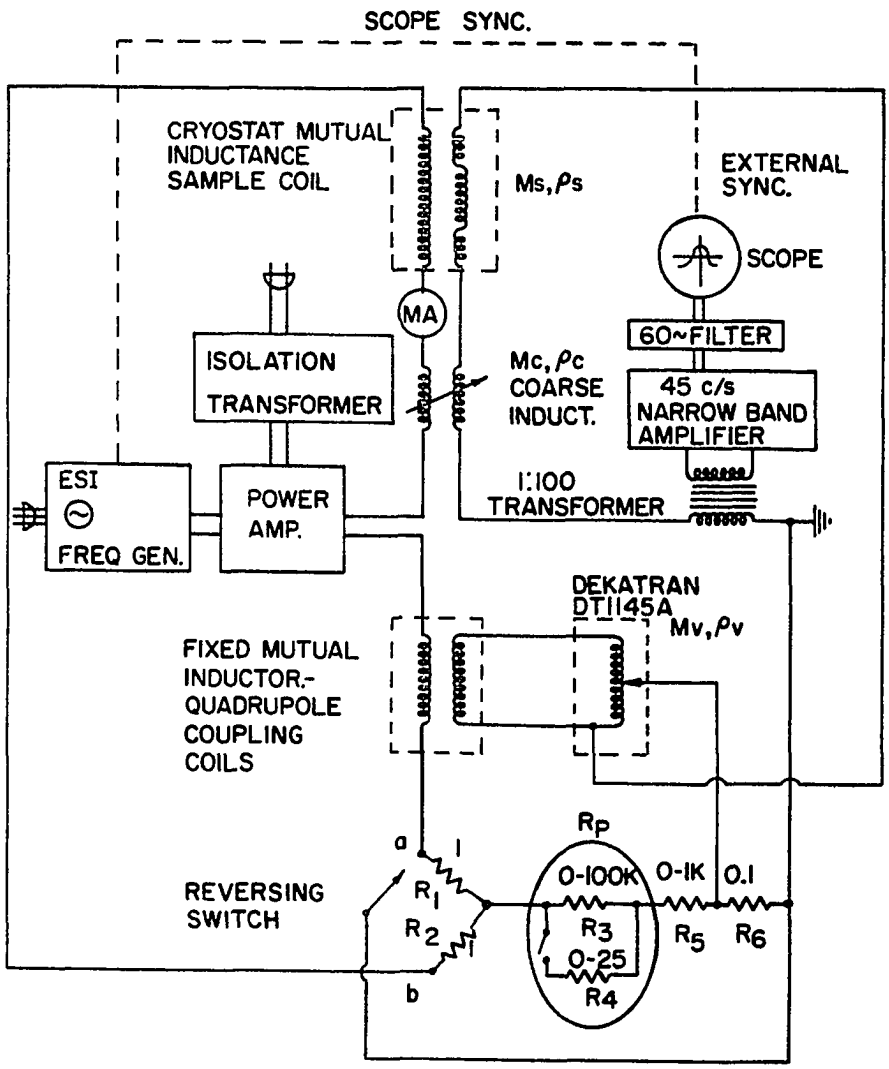

Fig. 24. Circuit diagram of "bridge" circuit

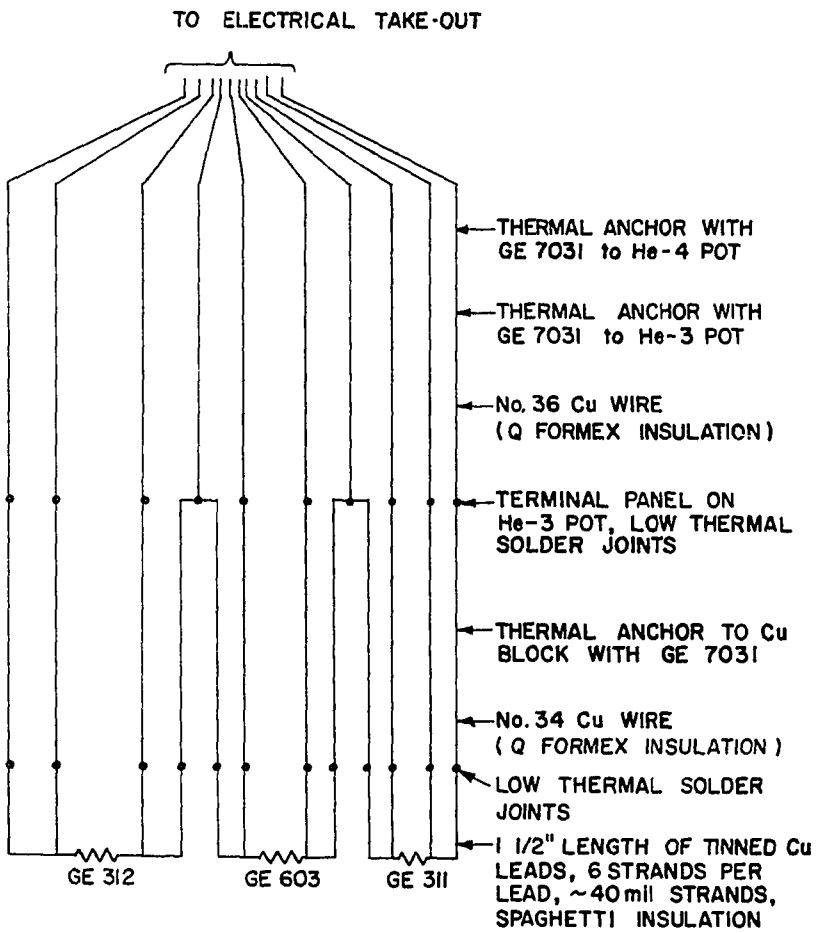

Fig. 25. Schematic view of thermometers and associated lead arrangement within BCG can of calibration apparatus

that described in section III A 7, and shown in Figs. 17 and 18.

C. Sample Preparation

1. Calibration of thermometers

The salt chosen for use as a standard thermometer in the range ~.45-2°K was cerous magnesium nitrate (CMN), $Ce_2Mg_3(NO_3)_{12}\cdot 24H_2O$. This salt is frequently chosen as a standard below ~1°K as has been discussed elsewhere (49,47).

The CMN was prepared by dissolving 89.357 grams of commercial $Ce(NO_3)_3$ and 103.424 grams of reagent grade $Mg(NO_3)_2\cdot 6H_2O$ in 244 ml of distilled water. The solution was filtered, the mother liquor being poured into Petri dishes and allowed to stand for a couple days. As the first crystals precipitated they were removed from the dishes and redissolved in distilled water. The resulting solution was again poured into Petri dishes and allowed to evaporate to complete dryness. The large white crystals that appeared were ground in a mortar. Silicone oil (Dow Corning 704) was added to the ground crystals as a binder, and the resulting mixture was packed into the nylon salt pill container (H, Fig. 21). About 3-4 cm^3 of silicone oil was used on the CMN in the container, and about 45 grams of CMN was packed into the container.

2. Heat capacity

The ReO_3 used for the heat capacity measurements was obtained from Physics Group VI, and had been prepared by vapor

transporting commercially obtained (City Chemical Corp.) ReO_3. A mass spectroscopic analysis of the ReO_3 used for the heat capacity measurements is compared against that of a sample of ReO_3 prepared by City Chemical Corp. in Table 6.

About 9 grams of crystalline vapor-transported ReO_3 was received from Physics Group VI. The crystals were randomly shaped chunks (with a mean width of ~1 mm), and had a maroon color with a metallic luster. The chunks were ground with a marble mortar and pestle to a consistency about that of fine sand. The ground ReO_3 was then placed in a Cu foil container and compressed into a pellet as follows. The Cu container was made by wrapping a rectangular piece of 1.5 mil Cu foil (~7/8" x ~1 5/8") around a brass rod (.492" ± .02" dia) to form a cylinder. One end of the cylinder extended ~1/16" beyond the brass rod. A circular piece of 1.5 mil Cu (~.49" dia.) was set on the end of the rod (inside the cylinder) and the edges of the Cu cylinder were crimped over to hold the circular piece in position. The brass rod plus Cu foil cylinder (now sealed on one end) was then inserted into a "1/2 inch" die. The brass rod was removed, leaving the Cu container in the die. The ReO_3 sample was added to the container until it was ~1/16" from being full. A second circular piece (~.49" dia.) of 1.5 mil Cu foil was placed on top of the sample, and the cylinder edges were crimped over. At this point 8.4874 ± .005 grams of ReO_3 had been loaded into a sealed cylindrical

Table 6. Mass spectroscopic analysis of ReO_3 samples

Element	ReO_3-1[a] (ppm)	ReO_3-2[b] (ppm)	Element	ReO_3-1 (ppm)	ReO_3-2 (ppm)
Be	≤1	≤.9	Ge	N.D.	N.D.
B	≤30	≤50	As	1	.4
F	4	.3	Se	N.D.	N.D.
Na	370	30	Br	N.D.	N.D.
Mg	20		Rb	N.D.	N.D.
Al	7	3	Sr	N.D.	N.D.
Si	50	10	Y	40	.6
P	1	3	Zr	N.D.	N.D.
S	≤50	≤10	Nb	≤10	<10
Cl	20	20-1000[c]	Mo	5	1
K	40	2	Ru	N.D.	N.D.
Ca	7	5	Rh	N.D.	N.D.
Sc	≤4	≤4	Pd	N.D.	N.D.
Ti	≤5	≤6	Ag	N.D.	N.D.
V	200	.3	Cd	≤.9	N.D.
Cr	20	2	In	N.D.	N.D.
Mn	5	.2	Sn	N.D.	N.D.
Fe	200	.6	Sb	N.D.	N.D.
Co	10	.1	Te	N.D.	N.D.
Ni	7	.06	I	N.D.	N.D.
Cu	60	.5	Cs	N.D.	N.D.
Zn	40	.9	Ba	N.D.	N.D.
Ga	≤ .2	N.D.[d]	La	N.D.	N.D.
Ce	N.D.	N.D.	Hf	N.D.	N.D.
Pr	≤.1	N.D.	Ta	N.D.	N.D.
Nd	N.D.	N.D.	W	N.D.	N.D.
Sm	N.D.	N.D.	Os	N.D.	N.D.
Eu	N.D.	N.D.	Ir	N.D.	N.D.
Gd	N.D.	N.D.	Pt	N.D.	N.D.
Tb	N.D.	N.D.	Au	N.D.	N.D.
Dy	N.D.	N.D.	Hg	N.D.	N.D.
Ho	3	3	Tl	N.D.	N.D.
Er	N.D.	N.D.	Pb	3	N.D.
Tm	N.D.	N.D.	Bi	N.D.	N.D.
Yb	N.D.	N.D.	Th	N.D.	N.D.
Lu	N.D.	N.D.	U	N.D.	N.D.

[a] ReO_3 made by City Chemical Corp.

[b] Vapor transported ReO_3.

[c] Inhomogeneous.

[d] N.D. - not detected.

(now ~3/4" in height by .495" ± .002" dia.) container (made of .3454 ± .0001 grams of Cu), and the container was positioned in a "1/2 inch" die. The die was then placed in a hydraulic press and a pressure of 500#/in^2 was applied for ~30 seconds. The resulting "pellet" that was extruded from the die was 1/2" in height and 1/2" in diameter. The top and bottom of the "pellet" were coated with Apiezon T grease (20 milligrams total), and the "pellet" was clamped in the sample holder (see Fig. 12) by placing it under the cross piece and tightening the screws.

IV. EXPERIMENTAL PROCEDURE

A. Calibration of Thermometers

1. Ge 603

Ge 603 was calibrated from ~1-28°K. The calibration equipment and experimental procedure have been described elsewhere (46).

2. Ge 311 and Ge 312

The thermometers Ge 311 and Ge 312 were calibrated from ~.45-2°K as follows. Three resistors (Ge 603, Ge 311, and Ge 312) were loaded into the Cu block (C, Fig. 21) and their leads connected as described in Fig. 25 and section III B 2. The rest of the calibration apparatus was then assembled as shown in Figs. 20 and 21. The He-3 and "inner" He-4 systems were evacuated to $\leq 10^{-3}$ mm Hg. The sample space was evacuated with the fore pump (shown in Fig. 6) for ~1 minute, then backfilled with ~1 atm of He-4. The He-4 dewar jacket was flushed several times with air, then backfilled with N_2 exchange gas to a pressure of ~1 cm Hg. The N_2 dewar (I, Fig. 2) was filled with liquid N_2, and an automatic refill device (made by Alco Valve Co.) was activated, which kept the dewar ~ full while the apparatus was allowed to cool overnight. The following morning liquid He-4 was transferred to the He-4 dewar (H, Fig. 2), and simultaneously He-4 gas was bled into the "inner" He-4 pot at a rate that was controlled by valve 1 (Fig. 5). This "back filling" of the "inner" He-4 pot was done with valves 1, 4, 5, 6, 8, 11 and 13 open, and the other valves

closed. After ~1/2 hour the He-4 dewar was full, and the pressure in the He-4 system as read on the manometer (see Fig. 5) had reached ~70-75 cm Hg. "Backfilling" was continued, and at ~76-78 cm Hg, the pressure in the inner He-4 system stopped rising, indicating that condensation of the He-4 in the "inner" pot (D, Fig. 2) had begun. The time was then noted and the He-4 flow rate was set to give ~50 cm^3 of liquid in 2 1/2-3 hours, after which the flow was stopped by closing valves 1, 5, 6 and 8 in Fig. 5). During the He-4 "backfill" all electronic instruments used were turned on for "warm up".

After the condensation into the "inner" He-4 pot was completed, the first "point" was taken. The chart recorder was engaged (and starting time noted) to record the output from the Fluke null detector (see Fig. 17). The resistance dialed on the variable standard resistor to produce a null on the recorder was noted on the chart paper for each thermometer. Simultaneously, mutual inductance readings were taken by another operator using the bridge circuit described in Fig. 24. Thus a "point" consisted of a series of null resistances for each thermometer (recorded on the strip chart) as a function of time, and a series of mutual inductance readings (proportional to the magnetic susceptibility of the salt pill (G, Fig. 21)) as a function of time. The time interval for a "point" averaged ~20 minutes.

After the first "point" (at ~4°K) the He-4 exchange gas

was pumped from the sample space until the pressure reached $\sim 10^{-5}$ mm Hg. The pressure over the "inner" He-4 bath was then reduced (and thus the temperature of the "inner" bath was lowered) by slightly opening valve 10 (Fig. 5). Within 15-30 minutes the thermometer resistance readings and the mutual inductance readings were relatively constant (to within $\pm$ .001 ^{o}K), suggesting that the thermometers and the salt pill were in thermal equilibrium (although it was possible that both had reached steady-state conditions at different temperatures). Once again a series of resistance and mutual inductance readings were taken as a function of time. During a "point", needle valve 10 (Fig. 5) was manually manipulated to keep the He-4 pot temperature constant. After some practice the temperature (as observed on the chart recorder) could be controlled to within one millidegree over a 15-30 minute period. In the above described fashion, "points" were taken in the range $\sim$1.5-4^{o}K over a period of $\sim$13 hours. Above $\sim 2^{o}$K only Ge 603 resistance readings were recorded, while in the range 1.5-2^{o}K Ge311 and Ge 312 readings were taken as well.

The following day the outer and inner He-4 baths were refilled as previously described in this section. Then valve 9 was completely opened (to lower the temperature of the inner He-4 pot to $\sim 1^{o}$K), and He-3 gas was slowly admitted to the He-3 system (see Fig. 4). Before admitting the He-3, valves 1-7, 10-15, 17, and 19-20 (see Fig. 4) were in the closed

position. For admission, valves 11-13 were first opened, then 14 slightly "cracked" such that all the He-3 was admitted after ~10 minutes. Within ~1 hour the He-3 had condensed in the He-3 pot, and had reached ~1.1°K (as read on the Hg manometer, Fig. 4). Temperatures were then controlled for the calibration "points" below 1°K by controlling the pumping rate on the He-3 pot. For most of the "points", valves 1-4, 6, 7, 9, 14, 15, 17, 19, and 20 were closed, valves 8, 10-13, 16, 18 and 21 were open and needle valve 5 was adjusted for control. For the lowest temperatures valve 6 was used for control.

In succeeding days the above procedure was essentially repeated until ~30 "points" had been taken between ~.45 and ~4°K. Ge 603 resistance readings were recorded from ~1-4°K, and Ge 311 and Ge 312 resistance readings recorded from ~.45-2°K. In the range ~.72°K to ~1.5°K, the vapor pressure over the liquid He-3 bath was measured at each of the "points", using a Wild cathetometer to read the manometers.

B. Heat Capacity Measurements

1. Addenda only

After completing the thermometer calibrations, the apparatus shown in Fig. 20 was converted to that shown in Fig. 2 (and described in more detail in section III A), with the exception that the sample holder (P, Fig. 8) did not contain the sample (O, Fig. 8).

When the dewars had been positioned as shown in Fig. 2,

the He-4 dewar (H, Fig. 2) jacket was flushed several times with air at room temperature, then backfilled with N_2 gas to a pressure of ~2-3 cm Hg. The sample space was evacuated to a pressure of ~1 micron, and backfilled to a pressure of ~2-3 cm Hg with H_2 gas. Evacuation of the He-3 and He-4 systems was begun. The N_2 dewar was filled with liquid N_2, and the automatic N_2 dewar refill device was activated.

After ~8 hours the sample holder had reached ~77°K, and evacuation of the sample space was begun. Liquid He-4 was then transferred to the He-4 dewar, and the pressure in the He-3 and inner He-4 systems was monitored to check that no leaks developed during the subsequent cooling. If no leaks developed, ~50-60 cm (of Hg) of He-4 was bled into the "inner" He-4 pot (as described in the previous section), and ~1-2 cm (of Hg) of He-3 gas was bled into the He-3 system (also described in the previous section). The apparatus was allowed to cool overnight in this configuration. After ~8 hours the sample holder had reached ~30°K, and the pressure in the sample space was ~10^{-5} mm Hg. The outer He-4 bath was refilled, and simultaneously He-4 gas was "backfilled" into the inner He-4 system (as described in the previous section). During the "backfill" the He-3 gas was bled into the He-3 system (using the procedure described in the previous section).

After ~80 cm^3 of liquid had been condensed in the He-4

pot, it was pumped to ~1°K within ~15 minutes by opening valve 9 (Fig. 5). The He-3 pot slowly followed the He-4 pot to ~1°K (by conduction through the pumping lines W and K, Fig. 8). After ~1 hour the He-3 pot reached ~1°K, and an estimated 3-4 cm^3 of He-3 had condensed in the He-3 pot. Pumping on the He-3 was then begun by opening valve 1 (Fig. 4) wide open. Within ~1 hour the sample holder reached ~.4°K.

The sample holder was then essentially thermally isolated by lifting it off the cooling platform (Q, Fig. 8), using the winch (Fig. 7). The lift off was usually done over a 2-4 minute period, and typically warmed the sample holder to ~.55 °K.

After lift off, heat capacity measurements were made using the "drift", "rate" technique (50). The temperature was allowed to drift for ~10-20 seconds (fore drift), then the heater-timer switch was activated to heat the sample holder. Below ~1°K heating periods were chosen to produce a change in temperature, ΔT, of ~.5%T. Above ~1°K, ΔT was usually ~1% T. After the heating period (~10-60 sec.) the temperature was again allowed to drift (after drift) for ~10-20 seconds, sometimes longer depending how long it took for the drift to become constant. The above procedure was then repeated until the highest desired temperature had been reached (~10°K for the sample holder).

During the heating period the voltage drop across the

heater, V_H, and the voltage drop across a standard resistor, V_{HS}, in series with the heater, were measured with a Leeds and Northrup K-3 potentiometer, using the circuit shown in Fig. 19.

During a drift the variable standard resistor setting was recorded, along with the Fluke sensitivity scale, and the thermometer current setting. Also the "zero" or null point on the Fluke was recorded from time to time using the zeroing switch on the Fluke.

After reaching ~10°K, the sample holder was set back on the cooling platform, cooled to ~.4°K, thermally "isolated", and another series of heat capacity points were taken. This procedure was repeated several times until ~100 points had been taken in the ~.5-5°K range.

2. Sample holder plus addenda

The above procedure was repeated after loading the ReO_3 sample in sample holder as shown in Fig. 8.

V. TREATMENT OF DATA AND RESULTS

A. Calibration of Thermometers

1. Ge 603

The objective of a Ge thermometer calibration is to obtain a relationship between the Ge thermometer resistance and temperature. The acquisition of the Ge 603 calibration data has been described elsewhere (46) in detail.

A "point" in the Ge 603 calibration consisted of a series of potentiometric voltage measurements (as a function of time) across several resistors (only Ge 603, Gr 618, and a standard resistor in series with Ge 603 and Gr 618 are of importance to this discussion). Germanium thermometer Gr 618 belonged to Physics Group II, and had been calibrated from 1-29°K as discussed in (46). In the range 1-4.2°K He-4 vapor pressure readings were also taken at each "point". During a "point" temperature was usually held constant to within $\pm$ .002°K.

The resistance of any thermometer, R_T, at time t, was obtained from Ohms law

$$R_T = V_T/i \qquad (7)$$

where V_T was the voltage across, and i the current through, a given resistor at time, t. The current at time t' was obtained from

$$i = V_S/R_S \qquad (8)$$

where V_S was the measured voltage drop at time t' across a standard resistor in series with the calibrated and uncali-

brated thermometer, and R_S was the known resistance of the standard resistor. Since the current was usually stable to .01% during a "point", and since V_T was usually measured within 60 seconds from V_S, the current from Equation 8 was usually substituted for i at time t in Equation 7. In some instances a linear interpolation was made between V_S measurements to obtain i at time t. Thus for a given "point", using Equations 7 and 8, one calculated R_{603} and R_{618} as functions of time. Then, using linear interpolation, R_{603} and R_{618} were found at some common time, t_c. The temperature at t_c was obtained from R_{618} using an equation of the form

$$\log_{10} T_{618} = \sum_{n=0}^{11} A_n (\log_{10} R_{618})^n \qquad (9)$$

using two sets of constants, (A_n) and (A_n'), which had been determined as described elsewhere (46). One set of constants, (A_n), was used in the range ~1-5°K. Using (A_n), $T_{618} = T_{58}$ (as measured by (46)) to within $\pm$ .001°K. T_{58} is the 1958 He-4 vapor pressure scale (51). The other set of constants (A_n') was used in the range 2.3-29°K, for which T_{618} ($=T_{CVGT}$) was a constant volume gas thermometer scale as explained in (46).

Using Equation 9, (A_n), and R_{618} at t_c, a set or R_{603}-T_{58} "points" was generated in the range 1-5°K. These R_{603} versus T_{58} values were then computer "fitted" to a polynomial expansion of the form

$$\log_{10}T_{603} = \sum_{m=0}^{M} A_m(\log_{10}R_{603})^m \quad M = 3 \text{ to } 10 \qquad (10)$$

where the constants A_m were found using a weighted least squares analysis discussed in (52). The value of M giving the best fit was chosen (as explained in (46)) by looking at deviation plots, and first and second derivatives of Equation 10 with respect to log R_{603}. For Ge 603, M = 10 gave the best fit. The root mean square deviation was 2.8×10^{-4} degrees. The values of A_m for M = 10 are given in Table 7.

Table 7. Fit constants for Ge 603 using Equation 10, M = 10

A_m	Value	A_m	Value
A_0	$2.191890972324 10\times10^{5}$	A_6	$1.27275093200542\times10^{2}$
A_1	$-2.61751067599731\times10^{5}$	A_7	$-8.52075623103587\times10^{0}$
A_2	$1.40215153834035\times10^{5}$	A_8	$3.73160573612446\times10^{-1}$
A_3	$-4.43685334850 30\times10^{4}$	A_9	$-9.65346998123353\times10^{-3}$
A_4	$9.18419242965567\times10^{3}$	A_{10}	$1.12020867849632\times10^{-4}$
A_5	$-1.29946910494100\times10^{3}$		

Using an analysis such as that described above, a set of fit constants was obtained to relate R_{603} to T_{CVGT} in the range 2.3-29°K. However, this scale was not used for any of the work reported herein and will not be discussed further.

2. Ge 311 and Ge 312

As mentioned in section III B 2, thermometers Ge 311 and Ge 312 were calibrated using the paramagnetic salt technique (53). In this case CMN was used as the salt. Basically this technique involved measuring the magnetic susceptibility, χ (or some quantity proportional to χ) of a paramagnetic salt obeying the equation

$$\chi = A'/T + B' \qquad (11)$$

where A' and B' are constants and T is thermodynamic temperature. A' and B', in principle, can be found by measuring χ at two known temperatures. In practice one usually measures the mutual inductance, M, produced by the paramagnetic salt in a "sample" coil, at various known temperatures T, since it can be shown (47) that

$$M = A/T + B \; . \qquad (12)$$

The M versus T data is then treated, using a linear least squares analysis, to find the best values of A and B. Once A and B are known, a measurement of M can be used to determine T. The salt pill can then be used as a standardizing thermometer by bringing other devices, such as a Ge resistor, into thermal equilibrium with the salt and simultaneously measuring M, and some property of the other device, such as the resistance, R, of a Ge resistor.

As discussed in section IV A 2, a "point" in the Ge 311 and Ge 312 calibration consisted of a series of mutual induc-

tance readings, made with the bridge circuit (Fig. 24) and a series of resistance measurements for Ge 603, Ge 311 and Ge 312, using the thermometer circuit (see Fig. 17). During a "point" the temperature was held constant to within ± .002 degrees, and null measurements were made with the comparator (as described in section III A 7). Thus thermometer resistance could be read directly from the variable standard resistor (VASTAR).

In the range 1-4°K, R_{603} at time t, was used with Equation 10 and the fit constants of Table 7, to determine T_{603} at time t. In the range .72-1.51°K He-3 vapor pressure measurements were also taken at each "point", using the manometers shown in Fig. 4 and a Wild cathetometer. The vapor pressure readings were corrected for room temperature, and elevation above sea level as outlined in (51). The corrections were ≤.001 degree. Thus, M versus either T_{603} or T_{He-3} or both was determined at 21 points in the region .720-4.192°K. The 4.192 point was thrown out because CMN is known (54) to deviate from the behavior described by Equation 11 at 4.2°K. Below ~1.3°K the T_{603} values were not used because they deviated systematically from the straight line relation expected from Equation 12. The remaining M versus T_{603} (and/or T_{He-3}) data were treated by computer to a linear least squares analysis. The results were

$$M = \frac{.042289(50)}{T_M} + .012985(45) \qquad (13)$$

where T_M is now the magnetic temperature associated with a mutual inductance reading M.

Using M readings at time t, and R_{311} readings at time t, and Equation 13, a table of R_{311} versus T_M was prepared. These data were treated to a similar least squares polynomial analysis as described for Ge 603. The resulting fit constants for use in the equation

$$\log_{10}T_{311} = \sum_{h=0}^{9} A_h(\log_{10}R_{311}) \qquad (14)$$

are given in Table 8. The root mean square deviation was $1.4\text{x}10^{-3}$ degrees.

Table 8. Fit constants for Ge 311 using Equation 14

A_h	Value	A_h	Value
A_0	$-1.5380161458169 95\text{x}10^{8}$	A_5	$3.011709059004921\text{x}10^{6}$
A_1	$2.4000631378079770\text{x}10^{8}$	A_6	$-3.466813369985113\text{x}10^{5}$
A_2	$-1.6631874171258640\text{x}10^{8}$	A_7	$2.563296005810836\text{x}10^{4}$
A_3	$6.7176130689242510\text{x}10^{7}$	A_8	$-1.104638071822687\text{x}10^{3}$
A_4	$-1.7427738428513 00\text{x}10^{7}$	A_9	$2.113950417668669\text{x}10^{1}$

The same analysis as described above was made for Ge 312, but Ge 312 developed a 10 megohm short to its case in the early heat capacity measurements and was replaced by Ge 311. Ge 311 and Ge 312 both came in the same shipment from Cryocal Corp. They had the same external dimensions and approximately

the same resistance at 4.2°K (~80 ohms). Ge 603 was 1050 ohms at 4.2°K.

B. Heat Capacity Measurements

The "drift-rate" method was used to determine C_{pm}, the mean constant pressure heat capacity, at $T_m(=(TF+TI)/2)$. TF is the temperature found by extrapolating the final temperature drift to the midpoint of the heating period, and TI is the temperature found by extrapolating the initial temperature drift to the midpoint of the heating period. C_{pm} is given by

$$C_{pm} = \frac{Q}{TF-TI} \tag{15}$$

where Q is the heat added (in this case by passing a current through the heater coil shown in Fig. 12) to the system to produce the temperature increase from TI to TF.

Q produced by a current i was calculated using the usual relationship

$$Q = (V_H)(i)(t) = (V_H)(V_{HS}/R_S)(t) \tag{16}$$

where t was the length of the heating period as measured by the timer (see Fig. 15), V_H was the voltage drop across the heater (Fig. 15), and V_{HS} was the voltage drop across the standard resistor (Fig. 15) of known resistance R_S = (1000.05 ohms).

TF was determined (using Equation 10 for Ge 603 and Equation 14 for Ge 311) from RF, the thermometer resistance

at the midpoint of the final temperature drift. RF was found from the equation

$$RF = ARF + (SF)(DF) \qquad (17)$$

where ARF was the approximate resistance at the midpoint of the final temperature drift, SF was the sensitivity (in ohms/division), and DF was the deflection "off balance" (in divisions). A typical heat capacity point as recorded on the Electronik-15 recorder (Fig. 17) is shown in Fig. 26 to illustrate ARF and DF. ARF is the VASTAR setting (see section III A 7) for the final temperature drift (ARF = 1500 ohms in Fig. 26), and DF is the number of divisions that ARF is "off balance" at the heating period midpoint (as shown in Fig. 26). SF, the sensitivity factor used to convert divisions off balance to ohms off balance, was rather difficult to determine for the electronic setup used because it turned out to be a function of thermometer current, Fluke scale setting, RF, DF, and direction of off balance (i.e., whether to the right or to the left of the null line shown in Fig. 26). Eventually a number of graphs were made up such as that shown in Fig. 27 from which the sensitivity was obtained. The points on the graph were determined (after the heat capacity data were taken) by substituting carbon resistors of known resistance in place of the thermometers (see Fig. 17) and reading the number of ohms on VASTAR required to produce a given deflection under the conditions stipulated on Fig. 27.

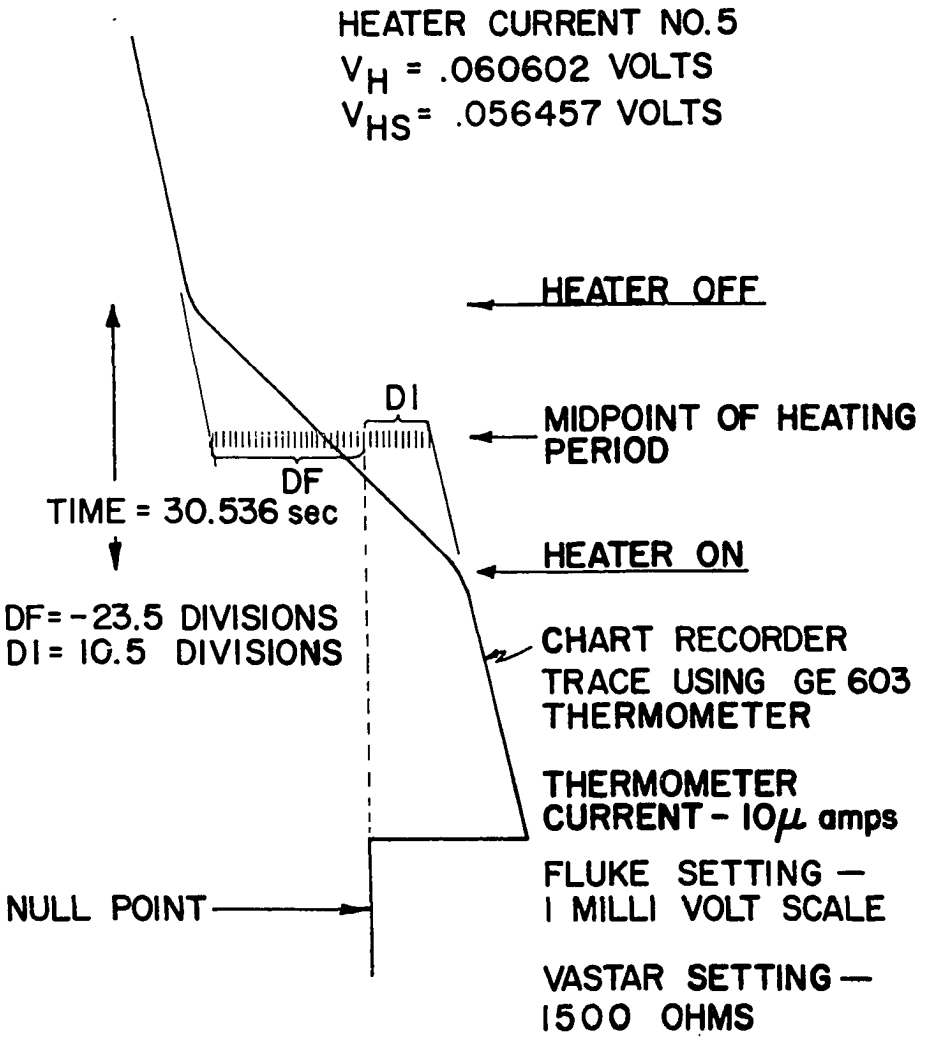

Fig. 26. Typical heat capacity data "point" as traced on the chart recorder

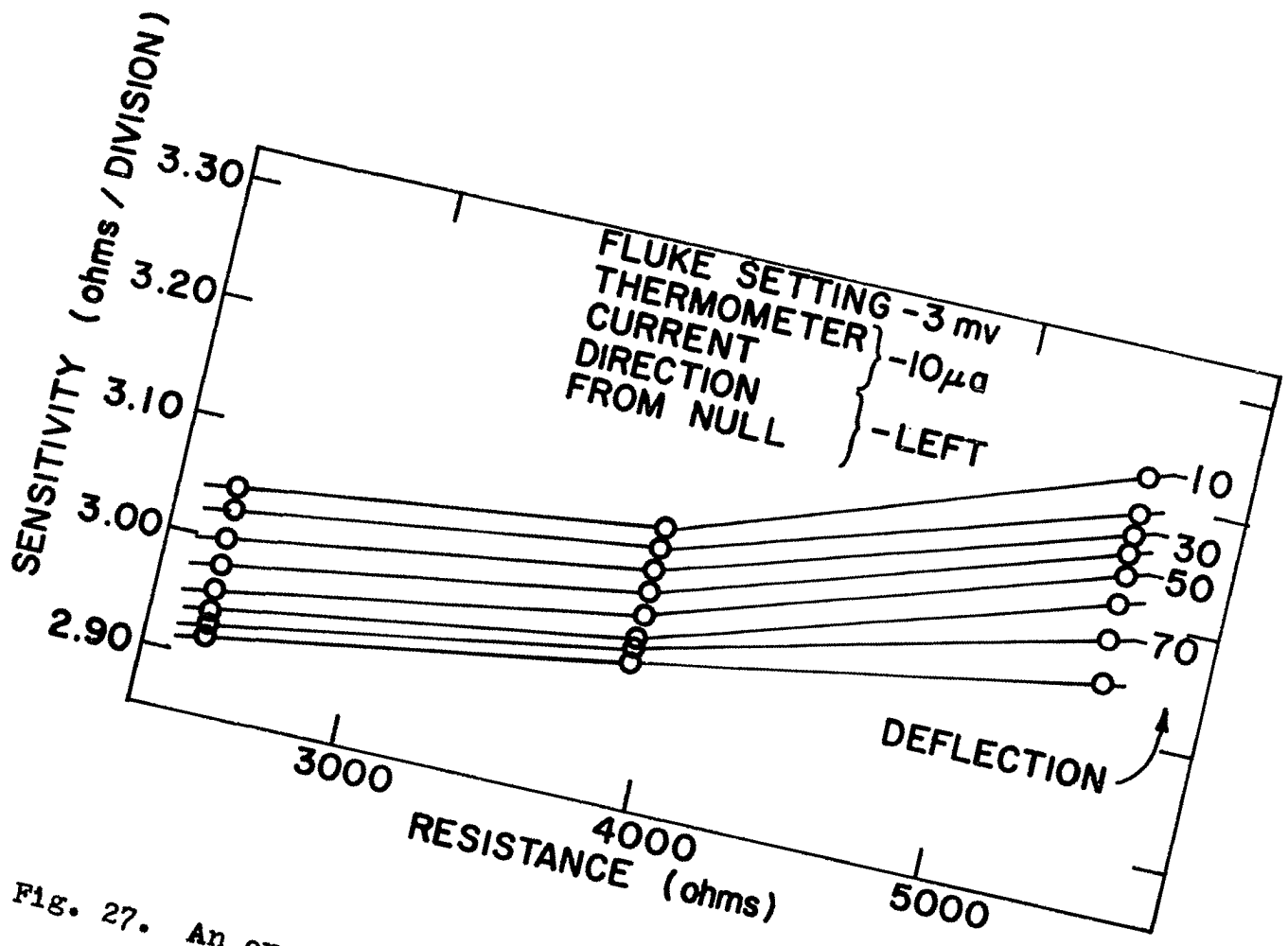

Fig. 27. An example of graph used to obtain sensitivity

TI was determined from RI, the thermometer resistance at the midpoint of the initial temperature drift, in the same manner as described for obtaining TF from RF.

A computer program was written to calculate C_{pm}, T_m, C_{pm}/T_m, and T_m^2 for each "point". The input parameters were the thermometer fit constants (from Tables 7 and 8), V_H, V_{HS}, t, ARI, ARF, SI, SF, DI and DF. The calculated results are shown in Fig. 28 where curve 1 shows the addenda measurements and curve 2 shows the addenda plus sample measurements. The peak at ~1°K was produced by the He-4 exchange gas used in the Ge thermometers and has been observed and discussed by others (18,55). The data from T_m^2 ~1.5 to T_m^2 ~18 $(°K)^2$ were treated using a linear least squares analysis to give a straight line fit for both curves. The heat capacity of the Cu foil used to enclose the ReO_3 sample was subtracted from the straight line fit for curve 2 using the equation

$$C_p = .6957T + .04783T^3 \text{ (millijoules/mole-°K)} \qquad (18)$$

obtained from reference (56), and the heat capacity of the Apiezon T grease (20 milligrams) used for thermal contact between the sample and sample holder was also subtracted from the fit for curve 2 using the equation

$$C_p = .00068T + .02714T^3 \text{ (millijoules/gram-°K)} \qquad (19)$$

obtained from reference (57). Higher order terms were ignored in Equations 18 and 19 because they contributed less than .1% to curve 2 at 4°K.

The equation for curve 1 was then subtracted from the corrected equation for curve 2 to give the equation for the heat capacity of ReO_3. The results fit the equation

$$\frac{C_{pm}}{T_m} = 2.85(\pm.15) + 2.54(\pm.10)\times10^{-2}T^2 \ \frac{(\text{millijoules})}{(\text{mole-degree}^2)} \ . \qquad (20)$$

The second peak shown in Fig. 28 (at T_m^2 $.3^\circ K^2$) was of unknown origin but appeared to be in curve 1 as well as curve 2, so was probably a temperature scale effect. Consequently, it did not appear to be a property of ReO_3, and was not treated any further.

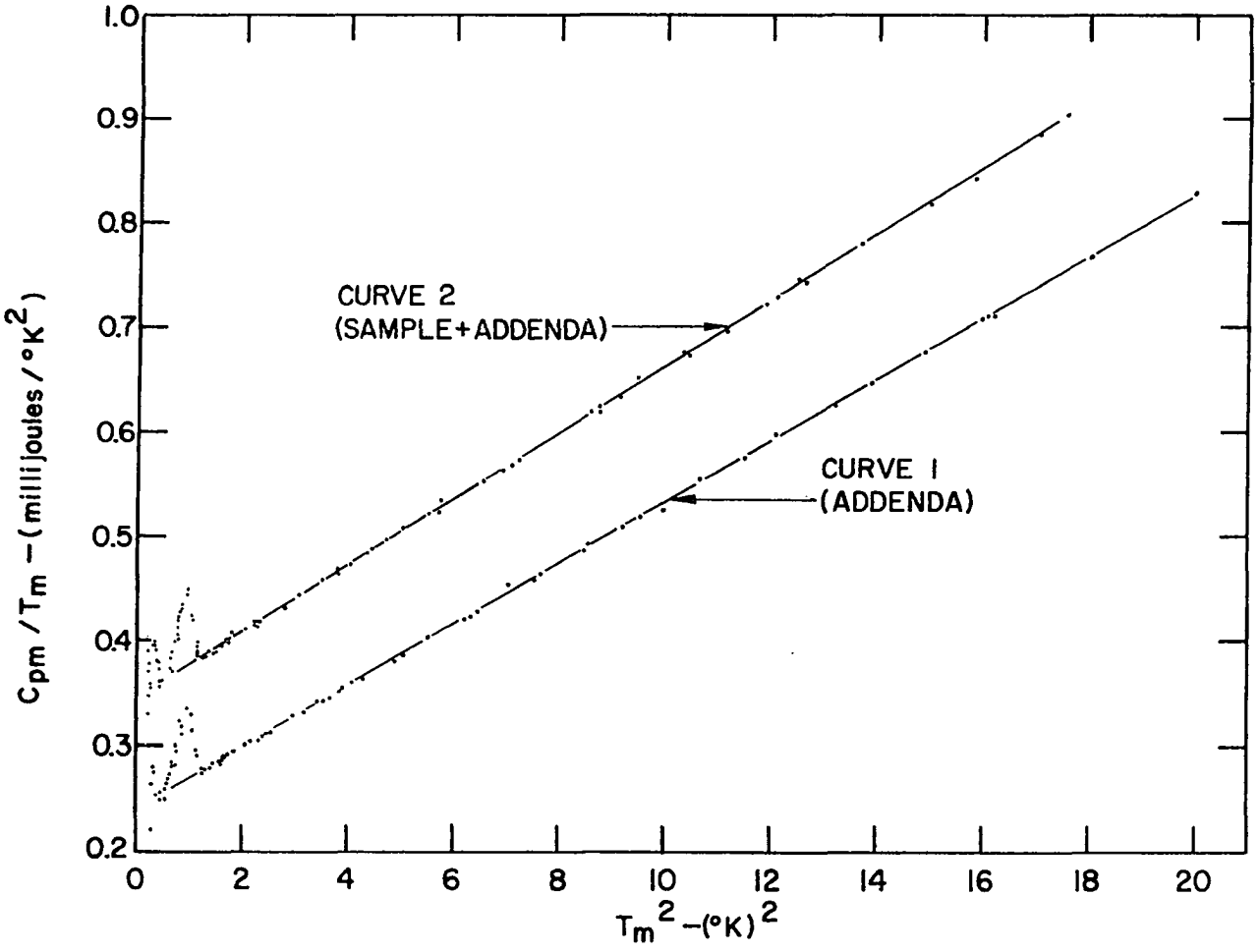

Fig. 28. Heat capacity results

VI. DISCUSSION

A. Thermometer Calibrations

1. Ge 603

The major sources of error in establishing $T_{603} = T_{58}$ are evaluated as follows. The Ge 603 temperature scale in the range ~1-5°K was prepared, as discussed in section V A 1, from R_{618} and Equation 9, using the set of fit constants (A_n).

As discussed in (46), R_{618} could be measured to $\leq$.01 ohms at ~4°K, which corresponded to $<1 \times 10^{-4}$ °K. The precision was estimated to be within .02%.

Equation 9, using (A_n), reproduced the T_{58} temperatures readings (that were used to generate (A_n)) to within 1 millidegree (RMSD = $\sim .6 \times 10^{-4}$ deg.). Hence, it is estimated that the use of a polynomial expansion, such as Equation 9, contributed to $\leq$ 1 millidegree error to the statement $T_{603} = T_{58}$.

The error in the T_{58} readings (made as described in (46)) was somewhat uncertain, but standard He-4 vapor pressure thermometry techniques (51) were used, so one might expect maximum deviations from T_{58} at any "point" to be of the order of 2 millidegrees and <1 millidegree on the average. However, below ~1.2°K the data is suspected to deviate systematically from T_{58} by as much as .004°K (See section VI A 2). T_{58} itself is now believed to deviate from the true thermodynamic scale by ~7 millidegrees at ~4°K, decreasing to ~2 millidegrees at ~1°K (52).

The use of Equation 10 and (A_m) in Table 7 to calculate T_{603} contributed on the average <1 millidegree error to the statement $T_{603} = T_{58}$ since the "fit" had a RMSD of ~.3 of a millidegree, and R_{603} could be measured, using the comparator circuit (section III A 7), to within .01 Ω (= ~.03x10^{-3} °K at 4°K) at all temperatures.

The stability of Ge thermometers to repeated thermal cycling between room temperature and ~4°K is another important factor in consideration of errors. Using thermal shocking techniques such as those described in (18), the stability of Ge 603 to thermal cycling was estimated to be ~1 millidegree. From the above considerations it was estimated that $T_{603} = T_{58}$ to within .0015°K in the range ~1.2-4.2°K, and deviated by as much as .004°K at 1°K.

2. Ge 311

The source of errors in the T_{311} scale are considered next. T_{311} was prepared, as described in section V A 2, from T_M (Equation 13). T_M was obtained from T_{He-3} and T_{603} as described in section V A 2. The estimated errors in T_{603} have been discussed in the previous section. The He-3 vapor pressures used to obtain T_{He-3} were read with a Wild cathetometer capable of .01 mm resolution. At ~.7°K, where the sensitivity is lowest, this corresponds to ~.8x10^{-3} °K. Thus T_{He-3} could be read to better than 1x10^{-3} °K. T_{He-3} is set up to join smoothly to T_{58}, and such was observed to be the case in the

Ge 311 calibration where the T_{He-3} vs M points fell on the same straight line (Equation 13) as the T_{603} vs M points, to within ~.2% from ~1.5-1.2°K. Below ~1.2°K the T_{603} vs M points deviated systematically from Equation 13 and were rejected in preparing the T_M scale.

The computer fit (Equation 14) between R_{311} and T_{311} left something to be desired however, with an RMSD of $\sim 1.4 \times 10^{-3}$ degrees, and deviations as large as 3×10^{-3} °K at ~1.5°K.

Another possible source of error to the T_{311} scale was that due to equilibrium problems between the salt pill (CMN) and Ge 311. Above ~.7°K it appeared that the thermal contact was satisfactory, as evidenced by the fact that when the R_{311} readings changed directions (i.e., when the temperature drift changed from warming to cooling or vice versa) the M readings followed within a few seconds. However, below ~.7°K, this correlation was not always obtained.

3. Power effects

There is always concern that the currents used in the thermometers will generate enough Joule heating to produce a temperature gradient between the Ge "chip" itself and the thermal contact with the surroundings outside the case (see Fig. 14). Therefore very low powers are used (as low as 10^{-10} watts). To check for a power effect, the thermometer current is reduced in steps, while holding the thermometer surroundings at a constant temperature, and resistance readings are

taken to see if a drop in temperature is indicated. Such checks were made with both Ge 311 and Ge 603 and the "power effect" was always less than $.3 \times 10^{-4}$ degrees between ~.45 and ~4°K. For Ge 311 the power used ranged from $.5 \times 10^{-9}$ watts at ~.5°K to $\sim 10 \times 10^{-9}$ watts at ~.85°K. For Ge 603 the powers used ranged from $\sim 4 \times 10^{-7}$ watts at ~1.25°K to 5×10^{-7} watts at ~2°K.

B. Heat Capacity

The results of the heat capacity measurements indicate that the electronic coefficient (γ, Equation 6) for ReO_3 is 2.85(mj/mol-deg^2) which can be compared with the values of 2.50 and 3.66 (mj/mol-deg^2) calculated using Equation 2 and values of $N(E_F)$ taken from Mattheiss (7) and Karian (5) respectively. The lower value would appear to be more satisfactory because it allows room for the electron phonon enhancement (58), which must be added to Equation 2. However, theoretical values of the electronic coefficient which are higher than experimentally determined values are not without precedent (33,34,35). To further compare the models it would be interesting to prepare some reduced ReO_3 samples and measure their electronic heat capacity. Assuming the rigid band case, Karian's work predicts that reduced ReO_3 should have a higher γ than ReO_3, while Mattheiss' model predicts the opposite.

Following the standard convention (29), the electron phonon enhancement factor, λ, can be calculated from

$$(1+\lambda) = \frac{3\gamma}{\pi^2 k^2 N a_o^3 G(E_F)} \qquad (21)$$

where γ is the experimental electronic heat capacity coefficient, k is Boltzmann's constant, a_o is the lattice constant (3.747Å), and $G(E_F)$ is the density of states at the Fermi surface per unit volume (taken, from a graph in (7), to be 14.43 states/ryd-unit cell). The value obtained of λ from Equation 21 was .14.

The coefficient, β (Equation 6), can be equated with the coefficient of the T^2 term in Equation 20. From β one can calculate the Debye temperature, θ_o, for ReO_3 in the range 1-4°K using the equation

$$\beta = 2.4\pi^4 nR(1/\theta_D)^3 \qquad (22)$$

where n is the number of atoms per formula weight (= 4 for ReO_3), and R is the ideal gas constant. The value of θ_D thus obtained was 312.9 deg.

Since the cubic perovskite reduced, $SrTiO_3$, is known to become superconducting at ~.25°K (59) the values of λ and θ_D were used to make an estimate of the superconducting transition temperature T_C of ReO_3 using the equation from (60)

$$T_C = \frac{\theta_D}{1.45} \exp - \frac{1.04(1+\lambda)}{\lambda-\mu(1+.62\lambda)} \qquad (23)$$

where μ is the pseudopotential (μ usually varies from ~.09-.15). Assuming a value of μ = .1, T_C is calculated to be $\sim 10^{-15}$ degrees for ReO_3.

VII. BIBLIOGRAPHY

1. Westrum, Edgar F., Furukawa, George T. and McCullough, John P. Adiabatic low temperature calorimetry. In McCullough, John P. and Scott, Donald W. eds. Experimental thermodynamics, volume I, pp. 133-211. New York, N.Y., Plenum Press, 1966.

2. Rulf, Donald C., Heat capacities of four rare earth trichloride hexahydrates from 5 to 300°K. Unpublished Ph.D. thesis, Ames, Iowa, Library, Iowa State University of Science and Technology, 1970.

3. Smith, Joan E., Magnetic susceptibility of cesium nickel chloride. Unpublished M.S. thesis, Ames, Iowa, Library, Iowa State University of Science and Technology, 1969.

4. Habenschuss, Michael, Ames, Iowa, Iowa State University, Magnetic susceptibility of nickel squarate, Private communication, (1970).

5. Karian, Harutun G., Tight-binding energy bands of perovskite type transition metal oxides, Unpublished Ph.D. thesis, Ames, Iowa, Library, Iowa State University of Science and Technology, 1969.

6. Galasso, Francis S. Structure, properties and preparation of perovskite-type compounds. New York, N.Y., Pergamon Press, 1969.

7. Mattheiss, L. F., Phys. Rev. 2nd series 181 (3), 987 (1969).

8. Onnes, H. K., K. Nederlandse Akademie van Wetenschappen, Amsterdam 11, 168 (1908).

9. Onnes, H. K. and Holst, G., K. Nederlandse Akademie van Wetenschappen, Amsterdam 17, 760 (1914).

10. Keesom, W. H. and Andrews, D. H., K. Nederlandse Akademie van Wetenschappen, Amsterdam 30, 434 (1927).

11. Phillips, N. E., Annales Academiae Scientiarum Fennicae 210A, 69 (1966).

12. Taconis, K. W., Prog. in Low Temp. Phys. 3, 153 (1961).

13. Hill, R. W., Prog. in Cryogenics 1, 179 (1959).

14. Roberts, T. R., Sydoriak, S. G., Phys. Rev. 98, 1672 (1955).

15. Hoare, F. E., Jackson, L. C. and Kurti, N., Eds., Experimental cryophysics, London, Butterworths, 1961.

16. White, G. K.. Experimental techniques in low-temperature physics, 2nd ed., London, Oxford University Press, 1968.

17. McCullough, J. P. and Scott, D. W., Eds., Experimental thermodynamics, Volume I. New York, N.Y., Plenum Press, 1966.

18. Swenson, C. A., Critical Reviews in Solid State Sciences 1, 99 (1970).

19. Gopal, E. S. R., Specific heats at low temperature, New York, N.Y., Plenum Press, 1966.

20. Gerstein, B. C., Heat capacity and magnetic susceptibility of thulium ethyl-sulphate. Unpublished Ph.D. thesis, Ames, Iowa, Library, Iowa State University of Science and Technology, 1960.

21. Keesom, P. H. and Bryant, C. A., Phys. Rev. Letters 2, 260 (1959).

22. Heller, P., Reports on Progress in Phys. 30, 731 (1967).

23. Giauque, W. F. and Fritz, J. J., J. Am. Chem. Soc. 71, 2168 (1949).

24. Keller, W. E., He-3 and He-4, New York, N.Y., Plenum Press, 1969.

25. Daybell, M. D. and Steyert, W. A., J. Appl. Phys. 40(3), 1056 (1969).

26. Finegold, L. and Phillips, N. E., Phys. Rev. 1969, 177(3), 1383 (1969).

27. Sorai, M., Kosaki, A., Suga, H. and Seki, S., J. Chem. Thermodyn. 1969, 119 (1969).

28. Trofimenkoff, P. N., Corbotte, J. P. and Dynes, R. C., Phys. Lett. 27A, (1968).

29. Clune, L. C. and Green, B. A., Phys. Rev. B 1(4) 1459 (1970).

30. Sommerfeld, A., Zeitschrift fur Physik 47, 1 (1928).

31. Bethe, H. and Sommerfeld, A., Handbuch der Physik, Berlin (Springer) 24, 333 (1933).

32. Kittel, C., Introduction to solid state physics, 3rd ed., New York, N.Y., John Wiley and Sons, Inc., 1968, Chapter 7.

33. Daunt, J. G., Prog. in Low Temp. Physics 1, 202 (1955).

34. Keesom, P. H. and Pearlman, N., Handbuch der Physik 14 (I), 282 (1956).

35. Parkinson, D. H., Rept. on Prog. in Physics 21, 226 (1958).

36. Mott, N. F., Adv. in Phys. 13, 325 (1964).

37. Wells, A. F., Structural inorganic chemistry, 3rd ed., London, Oxford University Press, 1962.

38. Goodenough, J. B., Rogers, D. B. and Ferreti, A., J. Phys. Chem. Solids 26, 2007 (1965).

39. Feinleib, J., Scouler, W. J., and Ferretti, A., Phys. Rev. 165, 765 (1968).

40. Marcus, S. M., Phys. Lett. 27A, 584 (1968).

41. Narath, A. and Barham, D. C., Phys. Rev. 176(2), 479 (1968).

42. Honig, J. M., Dimmock, J. O. and Kleiner, W. H., J. Chem. Phys. 50(12), 5232 (1969).

43. Neighbor, J. E., Review of Scientific Instruments 37, 497 (1966).

44. Cataland, G. and Plumb, H. H., J. Research Natl. Bur. Standards 70A, 243 (1966).

45. Dauphinee, T. M., Can. J. Phys. 31, 577 (1953).

46. Rogers, J. S., Tainsh, R. J., Anderson, M. S., and Swenson, C. A., Metrologia 4, 47 (1968).

47. Abel, W. R., Anderson, A. D., and Wheatley, J. C., Rev. Sci, Inst. 35, 444 (1964).

48. Rioux, F. J., Single crystal susceptibility study of one-dimensional antiferromagnetic interactions in $CsNiCl_3$. Unpublished Ph.D. thesis, Ames, Iowa Library, Iowa State University of Science and Technology, 1969.

49. Hudson, R. P., Cryogenics 9, 76 (1969).

50. Stout, J. W., in McCullough, J. P. and Scott, D. W., eds., Experimental thermodynamics, vol. I., P. 239. New York, N.Y., Plenum Press, 1966, Chapter 6.

51. Brickwedde, F. G., van Dyk, H., Durieux, M., Clement, J. R. and Logan, J. K., J. Research Natl. Bur. Standards 64A, 1 (1960).

52. Cetas, T. C., Magnetic thermometers between 1 and 20°K, Unpublished Ph.D. thesis, Ames, Iowa, Library, Iowa State University of Science and Technology, 1970.

53. Hoare, F. E., Kurti, N., and Jackson, L. C., Experimental cryophysics, London, Butterworths, 1961; and McCullough, J. P. and Scott, D. W., Experimental thermodynamics, Vol. I, New York, N.Y., Plenum Press, 1968.

54. Leask, M. J. M., Orbach, R., Powell, M. J. D. and Wolf, W. P., Proc. Roy. Soc. A272, 371 (1963).

55. Cochran, J. F., Shiffman, C. A., Neighbor, J. E., Rev. Sci. Instr. 37, 499 (1966).

56. Ahlers, G., Rev. Sci. Instr. 37, 477 (1966).

57. Westrum, E. F., Chow, C., Osborne, D. W. and Flotow, H. E. Cryogenics 7, 43 (1967).

58. Buckingham, M. J. and Schafroth, M. R., Proc., Phys. Soc. London Ser. A67, 828 (1954).

59. Schooley, J. F., Hosler, W. R., and Cohen, M. L., Phys. Rev. Letters 12, 474 (1964).

60. McMillan, W. L., Phys. Rev. 167(2), 331 (1968).

VIII. ACKNOWLEDGEMENTS

I would like to thank my major professor, Dr. Bernard C. Gerstein for his guidance, patience and moral support during my graduate work.

I would like to express my gratitude to Dr. William A. Taylor for his excellent advice, and assistance with the experimental work, and also Mr. William Shickell for his competent help with experimental problems.

Finally, my gratitude to my wife, Sue, for prodding me to the finish line.